Experimental Investigations on Carbon Fibre Reinforced SiC (C/SiC) during Rotary Ultrasonic Machining

A Dissertation

Submitted in partial fulfilment of the requirement for the

Degree of

Master of Engineering

In

Production Engineering

By

AKASH SHARMA

(801482001)

Under the guidance of:

Dr. Vivek Jain

Mr. Anil Kumar Jain

DEPARTMENT OF MECHANICAL ENGINEERING

THAPAR UNIVERSITY

PATIALA-147004, INDIA

JUNE-2016

भारत सरकार
अंतरिक्ष विभाग
विक्रम साराभाई अंतरिक्ष केन्द्र
तिरुवनन्तपुरम – 695 022
तार : स्पेस
टेलिफोन : 0471 -2563936
टेलेक्स : 0471 -2563446
फैक्स : 0471 -2705427

GOVERNMENT OF INDIA
DEPARTMENT OF SPACE
VIKRAM SARABHAI SPACE CENTRE
THIRUVANANTHAPURAM - 695 022
TELEGRAM : SPACE
TELEPHONE : 0471 - 2563936
TELEX : 0471 - 2563446
FAX : 0471 - 2705427

MATERIALS & MECHANICAL ENTITY
ADVANCED MANUFACTURING FACILITES

Date: 20-05-2016

CERTIFICATE

This is to certify that project titled "***Experimental Investigations on Carbon Fibre Reinforced Silicon Carbide (CSiC) during Rotary Ultrasonic Machining***" is a bonafide record of dissertation work carried out under my guidance and supervision at **Advanced Manufacturing facility** of the **Materials & Mechanical Entity** of **Vikram Sarabhai Space Centre, Indian Space Research Organization (ISRO), Thiruvananthapuram**, by **Mr. Akash Sharma, M.E.** student of **Department of Mechanical Engineering** of **Thapar University, Patiala, Punjab.** His attendance was regular and conduct & character was found good during the period.

Mr. Anil Kumar Jain,
Sci/Eng.-SE
AMF/IFF/MME
VSSC/ISRO

इसरो ISRO

भारतीय अंतरिक्ष अनुसंधान संगठन
INDIAN SPACE RESEARCH ORGANISATION

CERTIFICATE

I hereby declare that the thesis entitled "**Experimental Investigations on Carbon Fibre Reinforced Silicon Carbide (C/SiC) during Rotary Ultrasonic Machining**" is an authentic record of my study carried out as requirements for the award of the degree of **Master of Engineering in Production Engineering** at **Thapar University, Patiala** under the supervision of Dr. Vivek Jain, Assistant Professor, Mechanical Engineering Department, Thapar University, Patiala and Mr. Anil Kumar Jain, Scientist-SE, Indian Space Research Organization (ISRO), Vikram Sarabhai Space Centre, Trivandrum during May 2016. The matter embodied in this report has not been submitted in any part or full to any other university or institute for the award of any degree.

Akash Sharma

Date: 05/07/2016

This is to certify that above statement made by the student concerned is correct to the best of our knowledge and belief.

7/7/16

Dr. VIVEK JAIN

Assistant Professor,

Mechanical Engineering Department,

Thapar University, Patiala-147004

Mr. ANIL KUMAR JAIN

Sci/Engg.-SE, AMF/IFF/MME

Vikram Sarabhai Space Centre

ISRO, Trivandrum-695022

Countersigned by

Dr. S.K. MOHAPATRA

Professor & Head,

Mechanical Engineering Department,

Thapar University

Patiala-147004

Dr. S.S Bhatia

Dean of Academic Affairs,

Thapar University

Patiala-147004

ACKNOWLEDGEMENTS

I would like to express a deep sense of gratitude and thank profusely to my guides **Dr. Vivek Jain,** Assistant Professor, Mechanical Engineering Department, Thapar University, Patiala and **Mr. Anil Kumar Jain,** Scientist-SE, Indian Space Research Organization (ISRO), Vikram Sarabhai Space Centre, Trivandrum for their sincere & invaluable guidance, suggestions and attitude, which inspired me to submit thesis report in the present form. Their dynamism and diligent enthusiasm have been highly instrumental in keeping my spirits high. Their flawless and forthright suggestions blended with an innate intelligent application have crowned my task with success.

I am also thankful to **Dr. S.K. Mohapatra,** Professor and Head, Mechanical Engineering Department for his encouragement and inspiration for execution of the thesis work.

I am deeply indebted to my family for their inspiration and ever encouraging moral support, which enabled me to pursue my studies.

I am also very thankful to the entire faculty and staff members of Mechanical Engineering Department for their intellectual support and cooperation.

Akash Sharma

(Roll No.-801482001)

Dedicated to:

My lovely parents

Mr. M. C. Sharma & Mrs. Manju Sharma

Contents

List of Figures

List of Tables

List of Abbreviations

CMC	Ceramic Matrix Composite
C/SiC	Carbon fibre reinforced Silicon Carbide
CVI	Chemical Vapor Infiltration
RUM	Rotary Ultrasonic Machining
USM	Ultrasonic Machine
MTS	Methyltrichlorosilane
ℸ	Torque
DOC	Depth of Cut
Ra	Average change in Surface Roughness
MRR	Material Removal Rate
ANOVA	Analysis of Variance
DOF	Degree of Freedom
SS	Sum of Square

Abstract

Carbon fibre reinforced Silicon Carbide have widespread application in aerospace industry because of their superior properties like hardness, wear resistance, low density, high temperature resistance.

The composites were fabricated by the chemical vapor infiltration technique by using carbon fibre as reinforcement and silicon carbide as matrix material. Needling technique was used to create the fibrous preform.

However the use of C/SiC has been hindered seriously because of their poor machining characteristics. With an objective to improve the machining process of C/SiC composites, rotary ultrasonic milling of C/SiC composite of different densities was conducted. The effect of variation in material density, feed rate and axial depth of cut were studied by analyzing and optimizing the torque exerted during machining, material removal rate and change in surface roughness. Results shows that torque exerted during machining was increases with the axial depth of cut, feed rate and material density. Material removal rate was increases with the feed rate and axial depth of cut but it decreases with the material density. Change in surface roughness was reduces as the material density increases.

Scanning electrode microscope and EDS techniques were used to characterize the structure, fractured morphology in the fabricated matrix of C/SiC composites. SEM technique also used to examine the effect of rotary ultrasonic milling on the composite's structure.

Chapter1

INTRODUCTION

The engineering industry has been constantly evolving over the years through several innovations and inventions. The increase in the number of complex engineering applications has led to the development of many advanced materials such as advanced ceramics, High Strength Temperature Resistant (HSTR) alloys etc. The modern engineering industries are constantly dealing with these advanced materials to transform them to suit the various applications. The process of transforming these materials involves various forms of material removal from them. The material removal from these advanced materials is a great challenge faced by the modern engineering industry.

Among the advanced materials, the ceramics are finding widespread application in aerospace industry because of their superior properties like refractoriness and wear resistance over metals. The most important characteristic of ceramics that possess difficulty in machining is the brittleness or the fragile nature of the ceramics which causes them to crack easily while machining. They are also prone to thermal cracking at high temperatures that arise during the machining process at the tool-work interface due to the high temperature gradient that develops in their structure.

Machining of material can be generally categorized into two categories i.e. conventional (traditional) and non-conventional machining. Conventional machining contains direct contact of workpiece and tool. Highly brittle and hard material are difficult to machine by conventional machining techniques such as turning, drilling, shaping etc.

Non-conventional machining process like rotary ultrasonic milling has various advantage over conventional technique while machining of ceramics. It provides decreased cutting force, lesser generation of heat and increase in tool life.

1.1 Composites:

Composites are defined as the material in which two or more constituents have been brought together. The nature and properties of the composites is determined by the interface between the components. The strength of the composites is generally governed by the adhesion force which either chemical, physical or combination of both.

1.2 Types of Composites:

1. Metal matrix composite
2. Polymer matrix composite
3. Ceramic matrix composite

1.2.1 Metal Matrix composite:

Metal matrix composite are the materials which are formed by the combination of a metal with a metal or any other material. Strength and wear of material improve by the reinforcement of metal matrix. Generally matrix is of lighter metal such as aluminum, titanium, magnesium etc.

1.2.2 Polymer matrix composite:

Polymer matrix composite are the combination of polymer Matrix with fibrous reinforcement dispersed phase. The density of PMC's are less than the metal and ceramics. They are corrosion resistive in nature and have high insulation.

1.2.3 Ceramic Matrix composites:

Ceramic matrix composite are the combination of ceramic fibre with the ceramic matrix. This was discussed deeply in further points.

1.3 Ceramic Matrix composites:

Fibre reinforced ceramic matrix composites have high toughness and high strength [1]. CMC's are formed by the combination of a ceramic fibre which was implant inside a ceramic matrix to generate a finished CMC part. They are plausible due to their application in the field of thermostructural requirements.

The carbon fibre reinforced silicon carbide (C/SiC) composite possesses excellent wear, oxidation and thermal shock resistance [2]. It is light weighted, contains high specific strength, low density and abrasion resistance [3, 4]. Due to their good mechanical properties it was widely used as high temperature structural material in airplane engine, heat exchangers, racing cars etc. [3] it was also used as excellent raking material in aerospace field only after to C/C composites. It was used by NASA as flat component on X Series space machines and also used in high temperature oven. [1, 5].

In the modern world, the efficiency of cars, turbine engines, airplanes is attributed on the development of ceramic based chamber which can combat much higher temperature (approx. 1500°C) as compared to their metallic counterparts (1000°C). ISRO is using C/SiC for making nosecap, wing leading edge and control surfaces of his aerospace vehicle RLV-TD (reusable launch vehicle-Technology Demonstrator) where temperature encountered much higher than other like silica tile.

1.4 Methods of Preparation of Ceramic matrix composite:

1.4.1 Polymer Infiltration and Pyrolysis (PIP):

In polymer infiltration and pyrolysis, initially pyrolysing of fibre preform was done in inert gas atmosphere at temperature more than 900°C. This pyrolysing convert the preform into porous preform. After this capillary force was used to infiltrate the molten matrix material in vacuum atmosphere at temperature more than 1450°C. But composites formed by PIP have weak fibre matrix interfacial bonding. So porosity of composite is quite high.

1.4.2 Reaction Bonding:

In reaction bonding technique, a multi-layer of two different material was formed by adding thin layers of these material by chemical reaction. After this these multi-layer material was placed inside the layers of substrate at low temperature. Since the temperature is low so degradation of fibre is very low. In this process, the densification was avoided so possibility of shrinkage is reduced. This method is not applicable for bonding of frames of micrometer size.

1.4.3 Hot Pressing:

In hot pressing, powder or compacted material was placed inside the die and at high temperature (more than 2000°C) uniform pressure was applied across the die. This will make the material hard. Main limitation of hot pressing is the shape of material. As die is required so it is only suitable for simple shapes. Making a new die for each shape is not commercially viable. It needs so much graphite molds which require lots of time for mold loading and stripping.

1.4.4 Chemical vapor infiltration (CVI):

In chemical vapor infiltration fibre reinforced composite was made by infiltrating matrix material at high temperature in reactive gases environment into the fibrous preform. This was discussed deeply further.

1.5 Chemical Vapor Infiltration (CVI)

1.5.1 Process:

Chemical vapor infiltration (CVI) is a reaction- forming process which used for making CMCs. CVI is a similar technique like chemical vapor deposition (CVD), the only difference is in the deposition. CVD is used for deposition process on hot bulk surface while CVI is for deposition on porous surface. In CVD the deposition of material was done by pyrolysing the gaseous pressure, on the external surface of a bulk substrate. Chemical vapor infiltration is also CVD but on the internal surface of a substrate. CVD is commonly used for augment substrate surface and to deposit conformal films where conventional techniques for surface modification are not competent. CVI is highly useful in atomic layer deposition process for depositing enormously thin layers of material

A CVI process is differ from physical vapor deposition (PVD) processes, such as reactive sputtering and evaporation. They involves adsorption of molecular and atomic species on the substrate. In CVI on the other hand, the chemical reaction of the precursor gases takes place both on the substrate and in the gas phase. Reactions can be infiltrated by higher frequency radiations like as UV (photo assisted CVI), plasma (plasma enhance CVI) or through heat (thermal CVI).

The CVI process are highly complex in nature and includes so many gas phase and surface reactions. This process contains a “boundary layer” i.e. a hot layer of precursor gases just above the substrate. The gas phase pyrolysis reactions which occurs inside the boundary layer plays an important part in deposition process. In thermal CVI process, the growth rate of the film is mainly dependent on the operating pressure of the CVI reactor, chemical composition and interaction of gas-phase and the temperature of substrate.

1.5.2 Functioning of CVI-

A CVI system contains following work-

1. Transportation and evaporation of precursors in the bulk gas flow area inside the reactor.
2. Gaseous by products and reactive intermediates are generated by the gas phase reactions of precursors inside the reaction zone of the reactor.
3. Reactants transportation on the surface of the substrate.
4. Adhesion of the atoms or molecules (i.e. Adsorption) of the gaseous reactants on to the surface of the substrate.
5. After that diffusion of surface on to the growth sites takes place.
6. Chemical reactions onto the surface and nucleation which leads toward the formation of film.
7. At last desorption and transportation of waste material i.e. remains of the decomposition outside the reaction zone.

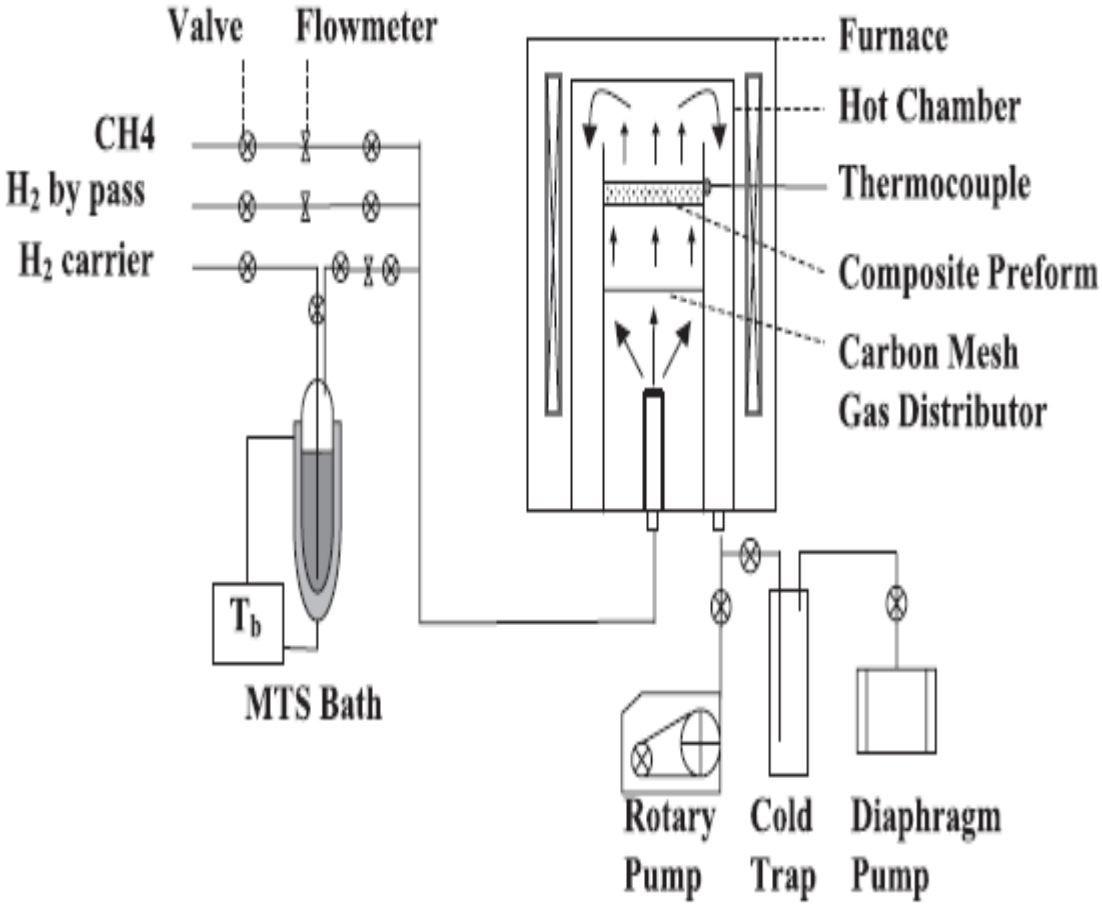

Fig. 1. 1: Schematic Representation of CVI system [4]

1.5.3 Processing of Fibre Reinforced Ceramic Matrix Composites via CVI process:

CVI process is very useful in fabrication of fibre reinforced ceramic matrix composites (CMCs) like C/SiC, C/C-SiC and SiC/SIC composites. In CVI process, a fibrous preform was prepared which was place inside the reactor of CVI. This preform work as the reinforcement material. Vapors or reactant gases were supplied inside the reactor that diffused into the fibrous preform (Fig 1.2). Composite material formed by the decomposition of these reactants, as they covered the void space between the fibers. In the composite, deposited material works as the matrix and fibrous preform act as reinforcement. The diameter of fiber increase with the progress in reactions (Fig 1.3)

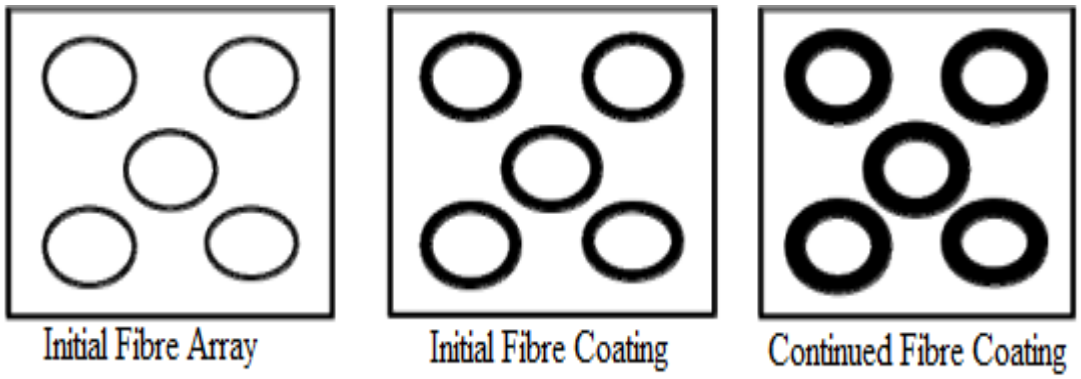

Fig. 1. 2: Chemical Vapor Infiltration Growth (1)

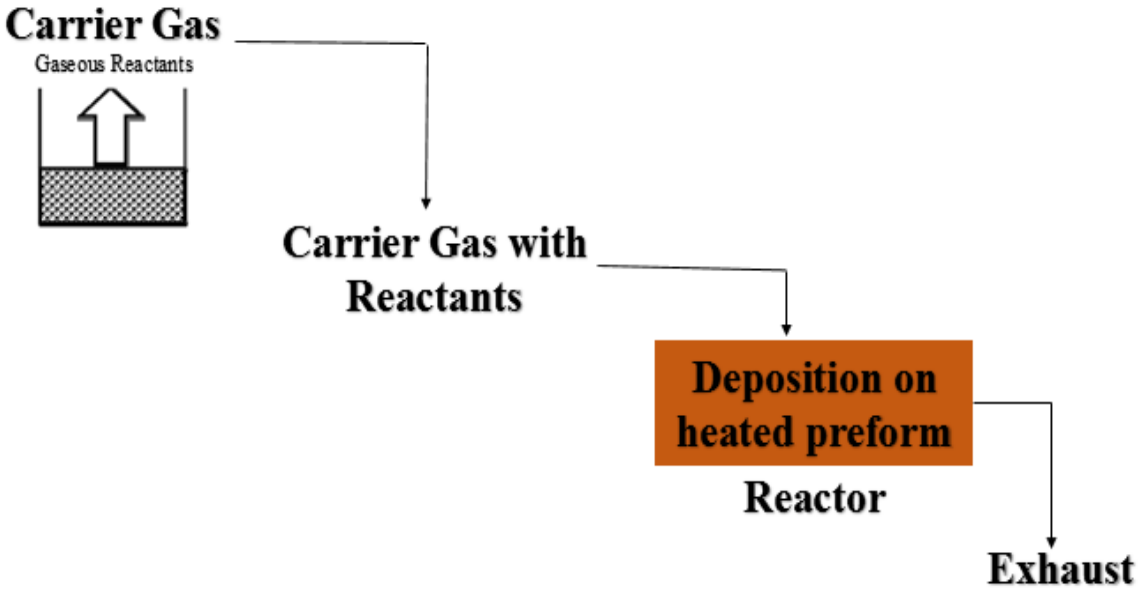

Fig. 1. 3: Stages in Chemical Vapor Infiltration Process

1.5.4 Processing OF CMCs:

Fibre reinforced fabricated by producing a dense ceramic matrix around carbon or silicon carbide filters. The fabrication of these dense matrix is mainly done by 3 techniques: using gaseous reactants (CVI: chemical vapor infiltration) or by using polymer reactants (polymer infiltration and pyrolysis), or by using molten elements reacting with the preforms (RMI: Reactive melt infiltration or LSI liquid silicon infiltration), or by using high pressure and temperature sintering of ceramic (HP-Sinter, High pressure-sinter process).

CVI process has following distinct advantages for the fabrication of CMCs:

1. A uniform coating was generated by CVI around each surface and fibre present in the preform.
2. Due to the presence of much lower temperature and pressure compare to other techniques, mechanical damage of fibre is less in CVI.
3. CVI provide purer surface compare to hot pressing.
4. Part generated by CVI has almost similar final shape as the desired one.
5. CVI enhances the mechanical properties such as hardness.
6. It increases the thermal shock resistance and corrosion resistance of the material
7. Materials densified by CVI does not require post treatment to eliminate the organics (as required in polymer infiltration process). Since, in CVI required atom or molecule reaches up to the smallest pores which was present in the preform.
8. Due to presence of low infiltration temperature, CVI produced low residual stress.

1.5.5 CVI Reactor:

Chemical vapor infiltration reactor works as the core body in CVI process. The diagram of reactor is shown in Fig 1.4. CVI reactor contains three important parts, which are:

a) A feed system

b) An effluent system

c) A heating chamber

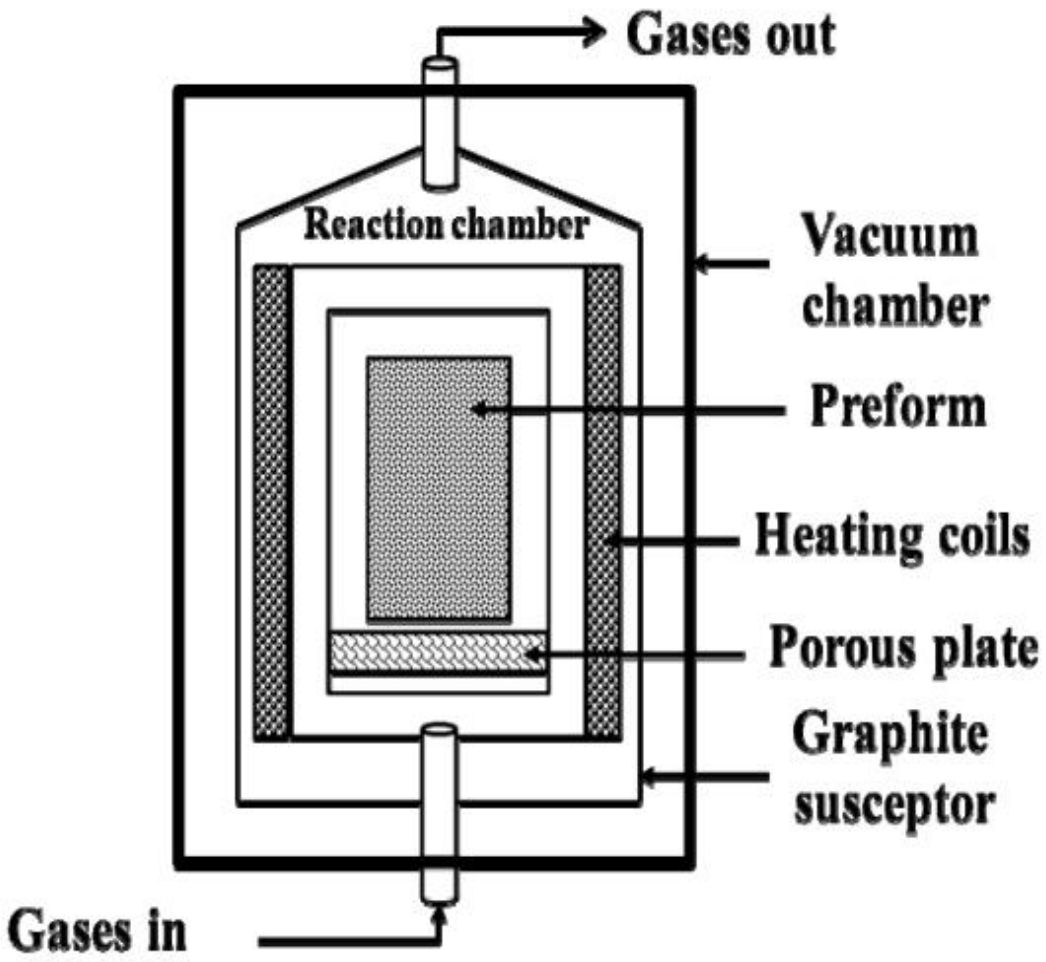

Fig. 1. 4: Chemical Vapor Infiltration Reactor (5)

1.5.6 Types of CVI process:

a) **Isothermal-Isobaric Infiltration-** It is the oldest hot wall technique which is widely used in industries as well as laboratories. In isothermal infiltration, gases are entered by the diffusion. These gases surrounds the whole porous substrate which was of fibre. It can densified many complex preforms together. The generated material has low residual stress and contains a uniform microstructure. Its main drawback is its slow processing time that sometimes more than 500h.

b) **Thermal Gradient-** in this process, heat is supplied only on one side of the fibrous structure. Reactant gases entered from the cold side and deposition will happen on to the hotter side. This creates a mobile reacting front where decomposition of vapor occur that produce the deposit.

c) **Pressure Gradient**-In pressure gradient CVI, the precursor gases are forced through the porous preform by applying a pressure gradient across the preform. This process can generate a ceramic matrix composite in very lesser time.

d) **Film Boiling-** In this process the preform is dipped into liquid precursor. The liquid precursor is recycled back after condensation due to which the efficiency of deposition is high at the cost of high power requirements.

1.5.7 Advantage of CVI:

- The processing temperature is low compare to other processes.
- it is able to fabricate complex structure composites
- Excellent mechanical behavior

1.6 CMCs for space applications:

The capability of SiC matrix composites as a structure of spacecraft was demonstrated at prototype level as "Hermes" (European space shuttle project). The maximum temperature lies their 800°C to 1600°C, during the ascent and re-entry phases of flight, and the structure withstood cyclic mechanical loading and thermal shocks under passive or ablative oxidizing atmosphere. C/SiC CMCs were proposed as a suitable candidate for the nose-cap of the X-38 which was designed to be a technology demonstrator of NASA for the crew return vehicle (CRV) from international space station ISS (Fig 1.5). During the re-entry phase the nose-cap of X-38 experience temperature up to 1750°C. European Space Agency (ESA) has proposed that C/SiC will be used for making all the Thermal Protection System (TPS) components of Intermediate Experimental Vehicle (IEV) [33].

Another area where high temperature capability of CMCs is useful is the thrust chamber of satellite thrusters. In existing satellite thrusters and LAM uses high temperature alloys, the permissible operating temperature is 1300°C whereas in C/SiC ceramic thrusters with suitable functionally gradient coating, the operating temperature is up to 1900°C which will enhance the impulse of thruster. Germany and China has already developed C/SiC nozzle extension and satellite thrust chambers. (Fig 1.6).

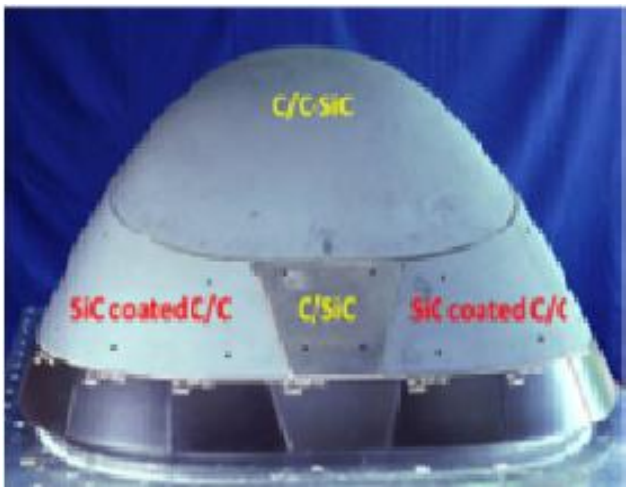

Fig. 1. 5**:** Nose-cap of X-38 (developed by NASA) (6)

Fig. 1. 6**:** 150 N C/SiC thruster (developed and tested by China) (7)

1.7 ROTARY ULTRASONIC MACHINING (RUM)

1.7.1 BACKGROUND OF RUM:

Continuous development and research has resulted in new materials, whose machining is very difficult, as hard materials, like tungsten, and titanium carbides, diamonds, hard steels, rubies, magnetic alloys. Another group of materials, such as silicon, ferrites, glass, quartz, germanium, sapphire, ceramics, corundum and some composites are difficult to machine because of greater hardness and brittleness. Ceramic matrix composites are also hard to machine such as carbon fibre reinforced silicon carbide C/SiC. The requirements for machining of these advanced materials have led to arise of non-conventional machining techniques like ultrasonic machine (USM).

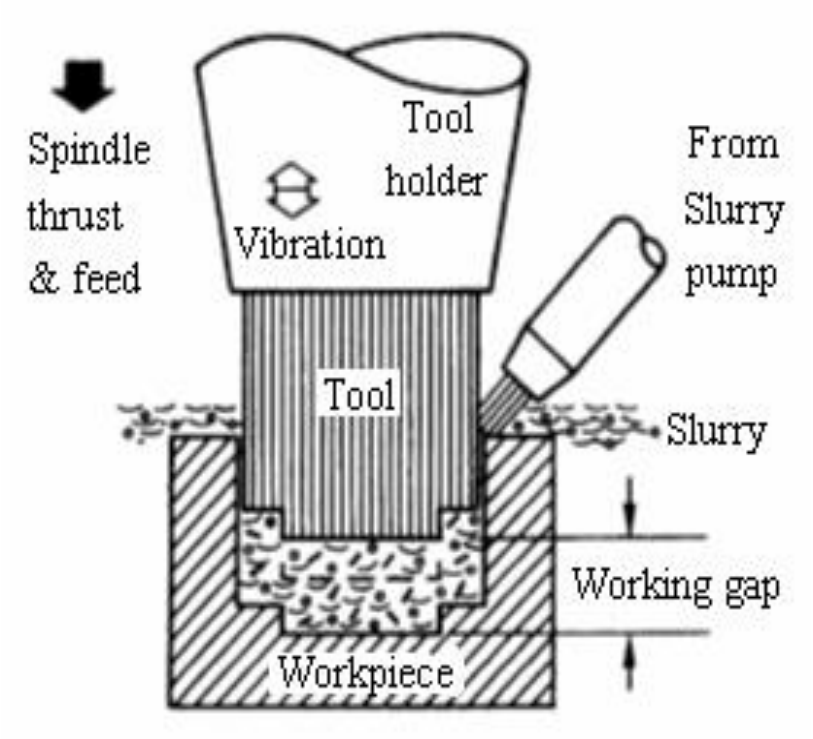

Fig. 1. 7: illustration of ultrasonic machine (13)

Fig 1.7 is schematic illustration of ultrasonic machine (USM). The tool will oscillates at a high frequency (>20 KHz) and is fed towards the workpiece with a high pressure. Abrasive slurry is supplied between the tip of tool and workpiece which consist of tiny abrasive particles and water. Material removal is in the form of small particles due to the continuous impacting of the abrasive particles onto the workpiece. But USM have some disadvantages also. The material removal rate and accuracy of work is low.

One modification of USM to overcome their disadvantage is rotary ultrasonic machine (RUM). It is a hybrid machining process, which combines the material removal process of ultrasonic machine and diamond grinding. The material removal rate obtained by RUM is higher than the USM as well as diamond grinding. In case of RUM, slurry is replaced by the abrasive bonded tool. A metal bonded tool diamond tool which is rotating as well as ultrasonically vibrating is fed into the workpiece with either a constant pressure or feed rate. Swarf is washed away by pumping the coolant through the core of drill. Coolant keeps the machine cool and also prevents the jamming of the drill that keeps the processing of RUM smooth and continuous. The process is illustrated in Fig 1.8.

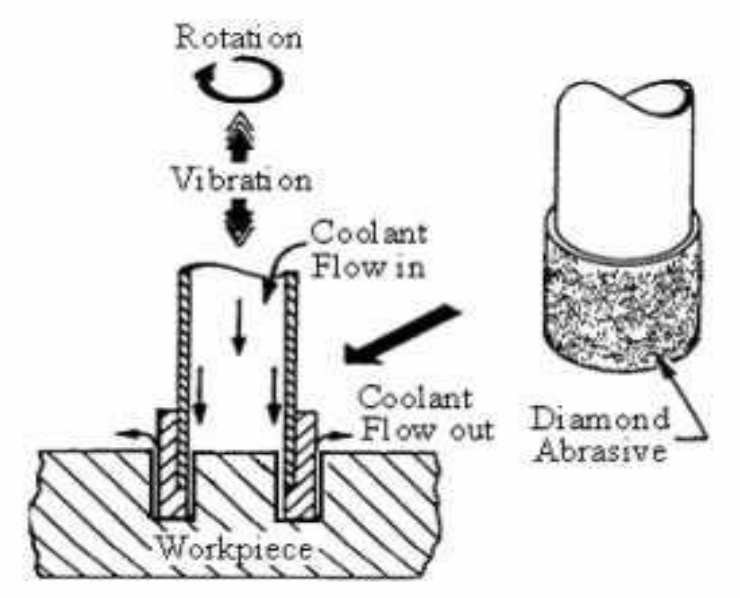

Fig. 1. 8: Illustration of Rotary ultrasonic machine (13)

Experimental results have shown that under similar condition RUM gives 6-10 times higher machining rate than conventional grinding process [8]. RUM is 10 times faster than the USM [Cleave 1976]. RUM can drill deep and small holes easily as compare to USM. RUM also provide low tool pressure and improved hole accuracy [Graff 1975, Stinson 1979].

1.7.2 EVOLUTION OF RUM:

RUM was developed as an improvement over ultrasonic machining. Unlike USM, instead of using the loose abrasive slurry, the diamond abrasives were impregnated into the rotating tool. Mainly RUM is used for drilling holes through brittle and hard materials. The development of RUM as a successor of ultrasonic machining (USM) is discussed in this section.

USM was patented in 1927 and has been continuously used in the industry since 1940 for machining materials with high brittleness and hardness. This process uses abrasive slurry, a mixture of diamond abrasives and a cooling fluid that is fed between an ultrasonically vibrating tool and the workpiece during machining. P. Legge developed RUM for the first time in 1964.

Continuous research also increase the application of RUM. Face milling of ceramics can also be done by this. RUM was firstly used for milling by pei et. al. in 1994.

1.7.3 Advantages of RUM over USM:

Some of the limitations of the ultrasonic machining were overcome in RUM. In the presence of the abrasive slurry, suspended abrasive particles and the escaping debris tend to erode the walls of the machined hole during flushing thus making it hard to hold close tolerances. Consequently, on abandoning of the abrasive slurry, RUM could be extended to a wider range of applications. Literature reported that RUM was capable of machining ten times faster then USM under same conditions. A low tool pressure and superior surface finish obtained by RUM compare to USM.

Chapter Organization:

CHAPTER 1: It contains the basic information about the composites and their types, chemical vapour infiltration process and rotary ultrasonic machining.

CHAPTER 2: It contains a literature study on the fabrication and machining of ceramic matrix composites. Finally the literature gap devised based on the gaps identified on the past work. This chapter extends the problem formulation, the objective of the present study and design of the present methodology.

CHAPTER 3: This chapter contains the fabrication of C/SiC composite and their properties, experimental set up, input and output parameters. The experiments planned according to 'design of experiment' are discussed in this chapter.

CHAPTER 4: This chapter contain the overall brainstorming over the effect of input parameters on the performance characteristics and thus the results have been postulated.

CHAPTER 5: Conclusions are explained along the groundwork of the present work in this chapter. Further, future scope in the field of rotary ultrasonic machining of C/SiC composite is also suggested in the same chapter.

Chapter-2

LITERATURE SURVEY

2.1 Literature Review:

This chapter focuses onto the latest development and investigation taken place in field of ceramic matrix composites. In the past years a lot of work has been done to fabricate and machining of ceramic matrix composites.

The literature review has been divided into two parts. First part is concern with the fabrication techniques of Carbon fibre reinforced silicon carbide. Second part has literature review related with machining of ceramic matrix composites.

2.1.1 Fabrication techniques of Carbon fibre reinforced silicon carbide:

J. C. Bae et al [3] uses the polymer infiltration and pyrolysing method for fabrication of C/SiC. Polycarbosilane (PCS) infiltrate was melted at high temperature and at 350°C heat treatment it totally infiltrate the carbon fibre preforms. This heating removes all low molecular weight component from PCS. Halogen (iodine) based curing was applied by the authors to enhance the ceramic yield, it becomes 91.7%. The initial density of C/SiC was 0.38g/cm^3 and after 6th iteration it becomes 0.42g/cm^3. Porosity was left only 13.6%.

Eun Ju Lee et al [4] uses hot pressing method for densification of high purity (99.998%) silicon carbide at 2100-2400°C under hot pressing pressure of 30-50 MPa. They observed that the densification of C/SiC was independent from initial particle size and hot pressing pressure affects it more compare to sintering temperature. Power law creep was considered as the mechanism of densification during hot pressing. The phase of hot pressed silicon carbide specimen remains preserve up to 2350°C.

Ke Zhao et al [2] introduced SiC nanowires into carbon fibre fabrics by pyrolysing of polycarbosilane precursor with the help of ferrocene catalyst before chemical vapor infiltration. Adding metallic catalyst increases the length of whiskers. Nanowires increases the final density of silicon carbide and also enhances the rate of densification of the CVI process. Open porosity reduces by the nanowires. Obtained preform takes 200h for densification. Authors also conclude that the high final density, densification rate and low

open porosity was due to the presence of extra surface which was given by SiC nanowires and change altered in their pores distribution.

Wen Yang et al [9] fabricated a SiC nanowires-reinforced SiC matrix composite by using chemical vapour infiltration (CVI) process. They prepared the composite preform by stacking 14 sheets of plain woven Tyranno-SA fibre cloth. This was located inside the vertical hot chamber of the CVI furnace. Before the nanowire growing process, the furnace was heated up to 1223K in vacuum chamber of lower than 0.1 Pa by rotary pump. For deposition of coating of carbon onto the fibres as interlayer between fibre and matrix, methane was used. For supplying of methane diaphragm pump was used in place of rotary pump.

Torben K Jacobsen et al. [10] has compare the mechanical properties of two Silicon carbide based matrix composite. Chemical vapor infiltration technique was used for the fabrication of these composites. One composite was C/SiC and another was SiC/SiC. In tension test, it was found that C/SiC undergoes up to third stage while SiC/SIC passes all four stages. Hysteresis and permanent deformation of C/SiC was large while SiC/SiC shows no hysteresis.

Byung Jun Oh et al. [11] uses the in-situ whiskers growing while fabrication of C/SiC composite through CVI. Methyltrichlorosilane and acetylene were used as the precursors. SiC is the matrix material and carbon tows are reinforcement. C/SiC produced with the help of in-situ whiskers has more density and less porosity than the C/SiC which are prepared conventionally.

Jingjiang Nie et al. [12] have tested the tensile behavior and microstructure of C/SiC which was fabricated by using CVI. Three regions were displayed in the strain-strain curve. One is long non-linear region, then a small linear region and at later stage a quasi-static region was found. Non-brittle fracture behavior was found because of non-linear tensile stress-strain curve.

T. Taguchi et al [13] has prepared the SiC/SiC composite which have multilayer interphase coating of SiC/C. their results shows that coating of SiC/C has higher tensile and flexural strength than only carbon interphase. In multi-layer SiC/C fibre pull out occurs

easily. Results also suggest that mechanical property of composite increased by using SiC/C.

Junqiang Ma et al [14] studies the tensile behavior and characterize the microstructure of 2.5D C/SiC composite which was fabricated by the CVI. In 2.5D C/SIC, composite has two and half dimensional architracture. Three different regions were found in the tensile test. One is long non-linear region, then a small linear region and at later stage a quasi-static region was found. In failure, multiple fracture of yarn was detected.

Sundar Vaidyaraman et al [15] fabricated the C/C composite by chemical vapor infiltration. They uses the T-3000 fibre for fabrication of preform. They initially fill the furnace with the argon and then heated it up to a certain temperature. After this precursors was flow into the preform. In the end infiltrated preform was cooled at room temperature and then remove it from the graphite preform holder. They conclude that higher density C/C composite was fabricated in very short duration by CVI. Uniform deposition was obtained on whole preform.

A.J. Caputo et al [16] uses the chemical vapor infiltration technique for fabrication of ceramic matrix composite. They prepared low density structure from SiC fibres by using vacuum forming technique. Infiltration on fibre structure was done by using Si_3N_4 and SiC matrix material. They conclude that time of infiltration reduces by using propylene as precursor. Only 8-12 hours were require to get the composite of less than 7% porosity.

H. Okuno et al. [17] study the effects of catalyst onto the C/C composite which was fabricated through CVI. They uses ferrocene as catalyst. When ferrocene was added in the liquid precursor, the densification rate is increases up to a temperature range of 1000°C. When this ferrocene is added inside carbon precursor, the texture of the deposited matrix has changed and it appears isotropic in nature.

2.1.2 Machining of CMC's:

Kai Ding et al. [5] performs the rotary ultrasonic machining of carbon fibre reinforced SiC of grain size 126 um and compares the result with conventional drilling. He uses sintered diamond core drill of outer diameter 6mm and inner diameter 5 mm. Drilling force and

torque used by RUM decreases by 23% and 47.6% respectively. He founds that RUM can produce high quality exit hole at higher feed rate but CD can give good hole quality at low feed rate and specific high spindle. RUM produces better machining quality since degree of tearing of hole determined by drilling force so hole exit is better at low drilling force. He also founds that surface roughness reduces 23% compare to conventional drilling. This is because of the reduction in size of chip. This reduction in chip size also suggest the less brittleness of C/SiC. The reduction percentage of torque and drilling force increased progressively with the spindle speed, while the change with the feed rate is very minor.

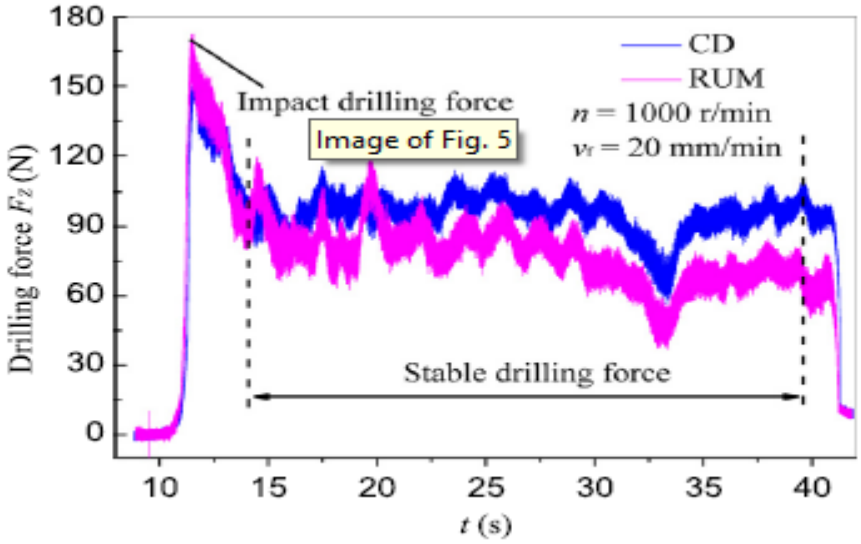

Fig. 2. 1: Comparison of Drilling Force between CD and RUM

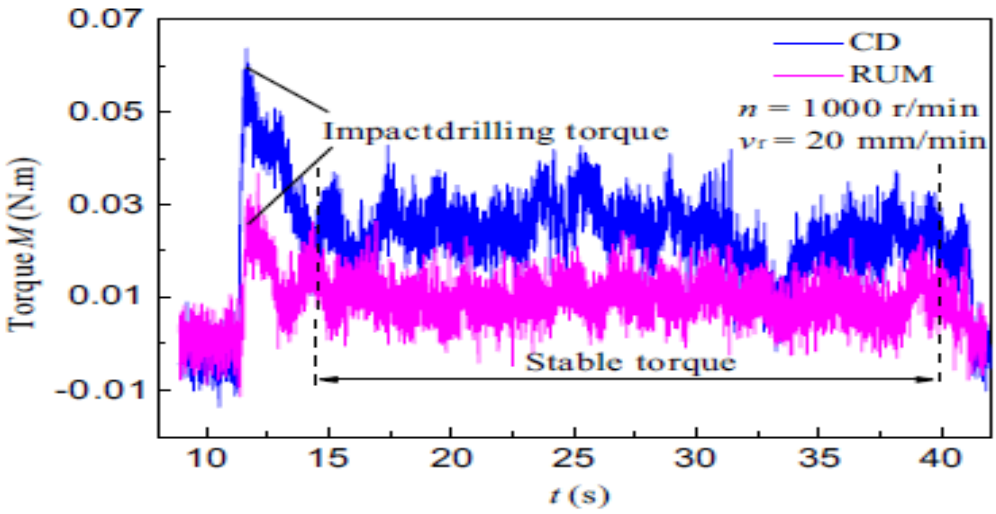

Fig. 2. 2: Compassion of Torque between CD and RUM

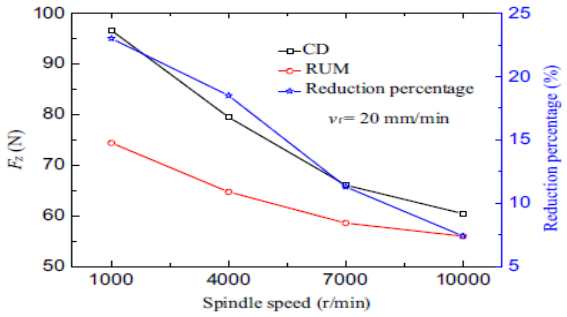

Fig. 2. 3: variation in drilling force in conventional drilling & RUM (Feed vs Spindle Speed)

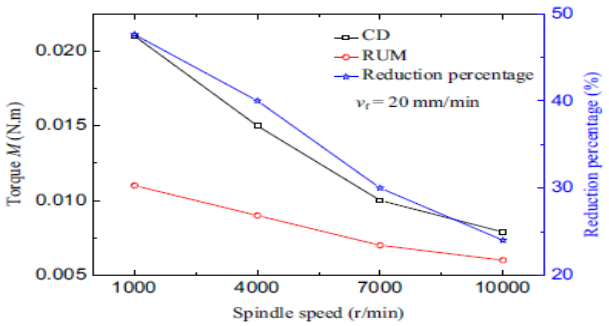

Fig. 2. 4: variation in drilling force in conventional drilling & RUM (Torque vs Spindle Speed)

H. Hocheng et. Al [1] fabricate the C/SiC by polymer pyrolysis route and heat treated it at 1800°C and use the ultrasonic drilling for machining work. 800W ultrasonic drilling machine at frequency of 20 KHz was used for conducting the experiments. A stainless steel tool of 4.51 mm outer diameter and 3.80 mm inner diameter was used. The density and flexural strength decreases while porosity increases by the heat treatment process. He uses feed rate of 0.12 mm/rev and finds the mrr by varying rotational speed i.e. 500, 1500 rpm. He experimentally founds that mrr increases with static load & grain hardness and hole clearance improves by increasing amplitude and deteriorate by increasing static load.

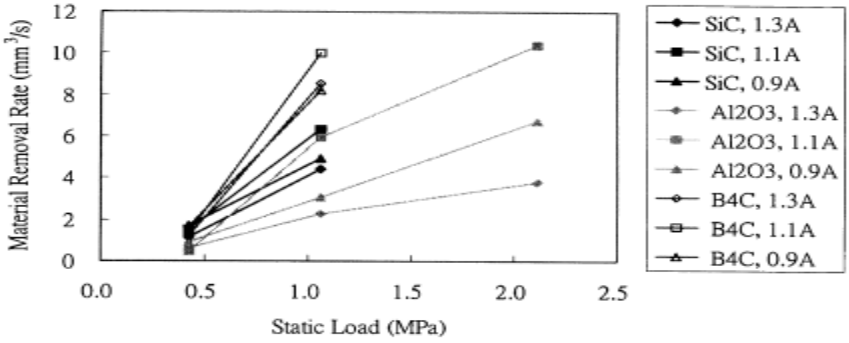

Fig. 2. 5: Influence of various grains on mrr

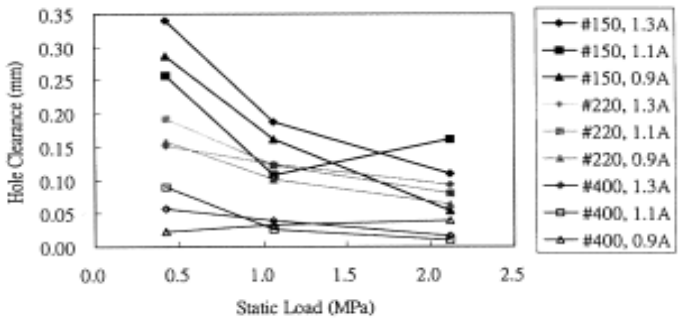

Fig. 2. 6: Influence of static load on hole clearance

M. A. Kadivar et al [18] adds ultrasonic vibration in drilling of Al/SiC metal matrix composites to reduce the burr size. The Al/SiC metal matrix composite contains 5 weight% SiC. They uses high speed steel drill tool which has coating of SiC for dry drilling operation. They prepares Al/ SiC by powder extrusion technique. The chosen vibration condition were 22 KHz with a fixed amplitude. The drilling process was carried out with three different feed rates of 0.08, 0.18 and 0.32 mm/rev and three spindle speeds of 125, 710 and 1400 rev/min. They found that during conventional drilling burr height was increased with the increase in feed rate and spindle speed but an optimum value was got for burr width. The ultrasonic vibration has provide smaller burr height and width in drilling of Al/SiC metal matrix composite. Their results shows that burr height was reduced by 83% and burr width by 24% by using ultrasonic assisted drilling compare to conventional drilling.

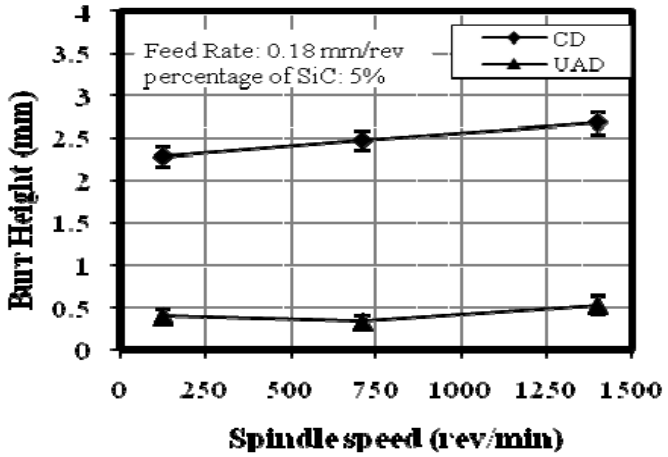

Fig. 2. 7: Burr height variation with spindle speed (at Feed rate = 0.18 mm/rev)

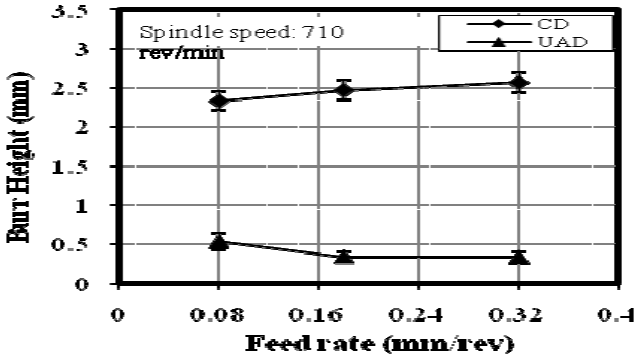

Fig. 2. 8: Burr height variation with feed rate (at Spindle Speed = 710 rev/min)

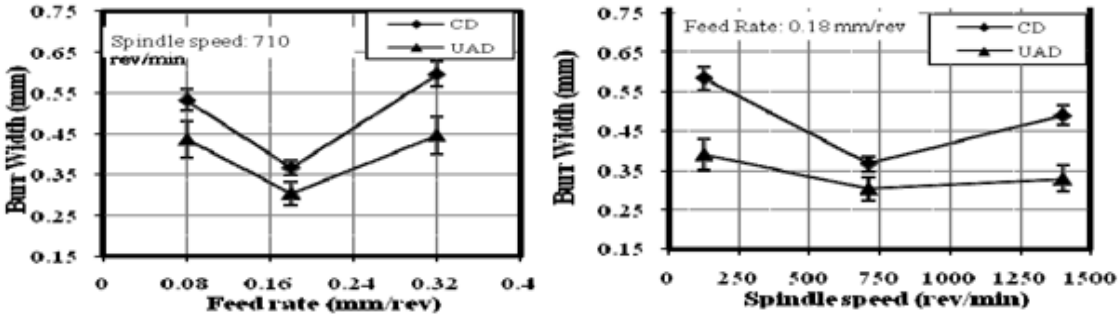

Fig. 2. 9: (a) Burr width variation with feed rate (at Spindle speed = 710 rev/min), (b) Burr width variation with spindle speed (at Feed rate =0.18 mm/rev)

M. Kadivar et al [19] investigate the effect of hole accuracy in ultrasonic drilling of Al/ SiC composite. Here they vary the amplitude and see the effect of cylindricity and circularity of hole. They found that ultrasonic assisted drilling provide approximately 60% improvement in Cylindericity and circularity compared to conventional drilling. This is because of the change in nature of cutting process and reduction in friction coefficient in UAD.

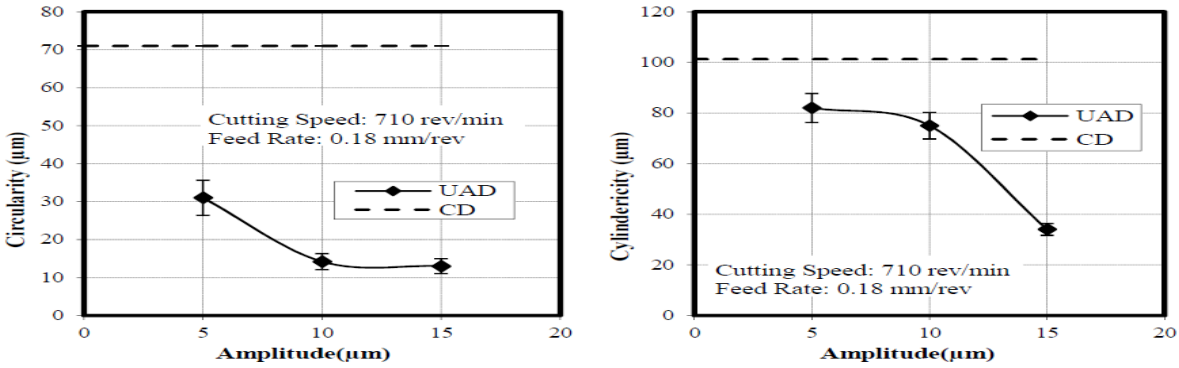

Fig. 2. 10: (a) Circularity vs amplitude, (b) Cylindericity vs amplitude

P. Mehbudi et al. [20] done the ultrasonic assisted drilling of fibre reinforced plastic (FRP) to reduce the delamination. They uses frequency of 22 KHz, amplitude of 5, 10, 15 um, spindle speed of 355, 710, 1000 rpm and feed rate of 50, 80, 110 mm/min. when they increases the amplitude, force decreases too much because chip breakage is expedited and duration of contact between workpiece and tool reduces so fracture of drilling reduces significantly. With the increment in feed rate, mrr increases and therefore cutting force also increases. While increasing spindle speed, thrust force decreases because increase in temperature makes the material softer. It was found that ultrasonic vibration reduces the delamination up to 50% in FRP.

Basem Abdo et al [21] optimizes rotary ultrasonic machining parameters during face milling of zirconia ceramics. The influence of RUM parameters amplitude, frequency, spindle speed, depth of cut and feed rate on the surface roughness was studied. They used diamond milling cutter of outer diameter 4mm and inner diameter 1.5 mm. the spindle speed was 2000, 4000, 6000 rpm, feed rate of 50, 100, 150 mm/min, vibration frequency of 20, 21.5, 23 KHz, power supply of 50, 60, 70% and depth of cut of 0.025, 0.05, 0.075 mm was used. They concluded that spindle speed and feed rate has largest impact on the surface roughness. Surface roughness is decreases by increasing spindle speed and/or decreasing feed rate. It increases slightly by increasing depth of cut. In their investigation minimum Ra value is 0.4295, which was at 6000rpm, 50 mm/min feed rate, 23KHz frequency, 60% power and 0.025 mm depth of cut.

V. Garcia Navas [22] investigate the effect of RUM on surface integrity of Al_2O_3-TiC-SiC ceramics, which was fabricated by the spark plasma sintering method (SPS). They use diamond milling tools of different grain size. They vary the cutting speed, feed rate, axial depth of cut (a_p) and frequency to find their effect on residual stress and surface roughness. While roughing operation, in face milling maximum mrr was found at 5000 rpm, 150 mm/min feed and a_p of 0.2 mm and in slot milling maximum mrr without workpiece damage was at 5000 rpm, feed of 300 mm/min and a_p of 0.3 mm. In finishing operation, during face milling best Ra was at 5000rpm, feed of 100mm/min and a_p of 0.05mm while in slot milling at 5000rpm, feed of 50 mm/min and a_p of 0.05mm. They finally concluded that lower compressive residual stress will be generated on increasing feed and decreasing

axial depth of cut. For lower Ra value diamond tool with smaller grain size will be used and for getting lower Ra value, increase the feed and reduce the axial depth of cut.

Yongsheng Liu et al [23] uses picoseconds laser for micro hole drilling of C/SiC of diameter 650 um. The C/SiC has been fabricated through CVI technique. C/SiC sample is of dimension 20×20×2 mm^3 & 20×20×3 mm^3 which is of 40% fibre volume fraction, density of 2gm/cm^3, porosity 10-20% and surface roughness value 2.0. The diameter of laser beam was 10um and rotational speed 40rev/sec. They uses different feeding speed and energy density of laser beam. With low energy density (0.51 J/mm^2) more debris generated in finished hole and circularity reduces. For thicker sample exit side boundary of hole left an irregular edge at low energy density and circularity reduces at exit side with increasing the feed. In case of 2mm thick workpiece, there is no effect of feed on hole quality.

J.W. Caroll et al [24] has done the laser machining of SiC/SiC composite by using CO_2 laser. High speed laser of 10 cm/sec gave smoother cut surface of Ra=4.96 um as compare to laser speed of 5 cm/sec which gave Ra of 5.83 um at 700 watt. The arithmetic average surface roughness found at both speed of laser was close to original value for material i.e. 4.87 um.

Chunhui Wang et. al. [25] have applied ultrashot pulsed laser for drilling film cooling holes and square holes in aero engine turbine blades fabricated of C/SiC. They uses CVI technique for fabrication of material of density 2gm/cm^3, porosity 10-20%. The specimen is made of size 20×10×3 mm. They found that small helical line spacing i.e. less than 0.05 mm was require to obtained a circular hole otherwise a donut shape can only be obtained because of Gaussian distribution of laser pulses, a certain degree of taper was present in the machined hole. Their results show that depth of hole reduces on increasing the scanning speed. At 100 mm/sec depth of hole was 700 um while at 200 mm/sec it was 500 um. This is because of reduction in time for debris to escape from the hole. There is no effect on diameter of hole of the scanning speed.

Lifeng Zhang et. al. [26] has done the grinding of C/SiC composites which was fabricated through CVI technique. The fibre volume fraction of material was 35-40 % and porosity

was less than 10%. They vary the rotational speed, feed rate and depth of cut to find out their effect on grinding force and surface roughness. At 1500 rpm grinding force in normal direction is 3 times of transverse direction. Results shows that on increasing the rpm, grinding force decreases while by increasing feed rate and depth of cut, the grinding force increase. The surface roughness also increases with increase in depth of cut and feed rate. Maximum surface roughness found in longitudinal direction and minimum in transverse.

T. wang et al [27] performs the high speed milling of Al/SiC/65p of mean particle size 5um aluminum matrix composites. They investigate the effect of feed rate, depth of cut and milling speed on the surface roughness and surface residual stress. Milling speed has maximum effect on the surface roughness than the feed rate. Surface roughness is minimum affected by the axial depth of cut. In case of residual stress, axial depth of cut has highest influence followed by milling speed and feed rate.

Basem Abdo et al [28] investigate the minimum cutting forces in Ti-6Al-4V alloy by using rotary ultrasonic machine. They uses vibration frequency, spindle speed, amplitude, coolant pressure, feed rate and depth of cut as input parameters. The diamond milling cutter of 4 mm outside diameter & 1.5 mm wall thickness and of D91 grain size was used. Results shows that vibration frequency of 25 KHz has minimum cutting force. Cutting force was increased with increasing coolant pressure, amplitude, feed and decrease with the spindle speed and depth of cut.

Z. C. Li et. al. [29] has conducted the feasibility study and experimental design while machining of ceramic matrix composites through rotary ultrasonic machine (RUM). They done the drilling on alumina and CMC workpiece. Diamond tool with mesh size of 140 which has outer diameter of 9.54 mm and inner diameter of 7.82 mm was used. They conclude that RUM has improved the mrr up to 10% and reduced the cutting force up to 50% comparing to diamond drilling. Hole quality was significantly affected by the interaction of spindle speed and feed rate. MRR was significantly affected by feed rate, spindle speed and ultrasonic power. While feed rate is predominant factor in behavior of cutting force.

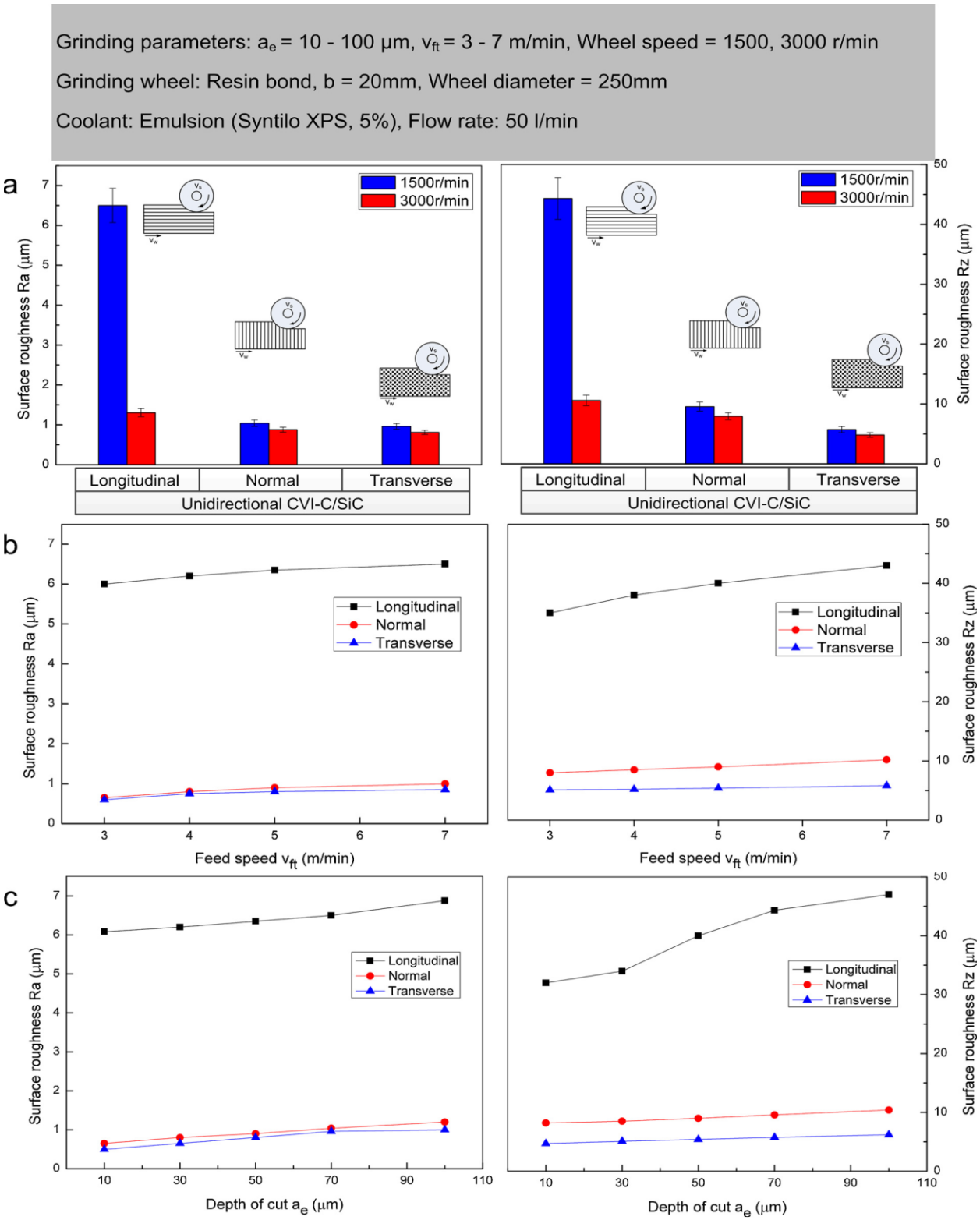

Fig. 2. 11: Variation of surface roughness with the workpiece material, the grinding process and (a) at cutting speed-5 m/min, a_e-70 µm; (b) at feed speed-1500 r/min (v_c-19.6 m/s), a_e-50 µm; (c) at depth of cut, v_s-1500 r/min (v_c-19.6 m/s), ~~¥~~$_{ft}$-5 m/min [26]

Mohsen Ghahramani Nik et. al. [30] has made the ultrasonic setup to do the grinding of Ti6Al4V alloy. They investigate the impact of ultrasonic vibration by taking frequency of 20KHz on to the Ti6Al4V alloy. Findings of their work shows that ultrasonic assisted grinding has reduced both tangential and normal cutting force. Ultrasonic vibration also improves the surface roughness up to 10% compare to normal grinding. Surface quality was better even at higher feed rate and depth of cut.

Erich Bertsche et. al. [31] has done the slot machining by using RUM and measure the process force and tool wear. They also compares the results with the normal grinding. Tool wear was reduced up to 36% and reduction in forces was found up to 20% compare to traditional machining. They also suggest that diamond tool of coarse grain size D181H with higher diamond concentration is best for the machining of ceramic matrix composites.

Yue Jiao et. al. [32] has conducted the rotary ultrasonic machining to study the impact on edge chipping while machining of ceramics. They uses diamond drill of 9.53mm outer diameter and 8.13 mm inner diameter. They vary the ultrasonic power, spindle speed, grain size and feed rate. Feed rate and spindle speed are the variables which have significant effect on the edge chipping. Smaller chip thickness was found at smaller feed rate and high spindle speed.

Chun-Yang Zhao et al. [33] has compared the cutting force while machining of K9 glass through conventional grinding and rotary ultrasonic machine. In their study they found that force generated through rotary ultrasonic machine is lesser than traditional diamond face grinding, drilling and side grinding. The maximum cutting force increases with increase in feed rate.

2.2 Literature Gap:

From the previous literature review it has been seen that C/SiC was machined by the grinding, milling and laser. Previous researcher also do the rotary ultrasonic machining of C/SiC. Based on the literature survey following analysis can be made and further gaps can be postulated.

- Machining of carbon fibre CMC's is very difficult because of its hard and brittle nature.
- Picoseconds laser does not provide smooth surface at low energy density.

- Ultrasonic pulsed laser is commercially not good because of requirement of small helical line spacing.
- Depth of machining in ultrasonic pulsed laser reduces on increasing the scanning speed.
- Previous attempts have been made on studies of mechanical properties of C/SiC but very few studies have been made on the machining characteristics.
- No work has been reported on comparing the machining of C/SiC of different densities.
- To provide an alternative of grinding as C/SiC was generally machined by grinding for making aerospace products.

2.3 Problem Formulation:

Rotary ultrasonic machining can be a high potential candidate for machining of ceramic matrix composites which are very hard in nature.

Thus, in the present study all the shortcomings of previous work were identified from a comprehensive literature survey and an attempt has been made for **"Experimental investigations on carbon fibre reinforced Silicon Carbide (C/SiC) during Rotary ultrasonic machining"**.

2.4 Objectives:

- To fabricate the C/SiC composites of different densities through CVI process
- To investigate and analyze the effects of various process parameters on performance characteristics of the RUM process.
- To optimize the process parameters by using Taguchi Method.
- To characterize the samples using SEM, EDS and Talysurf.

2.5 Work Plan:

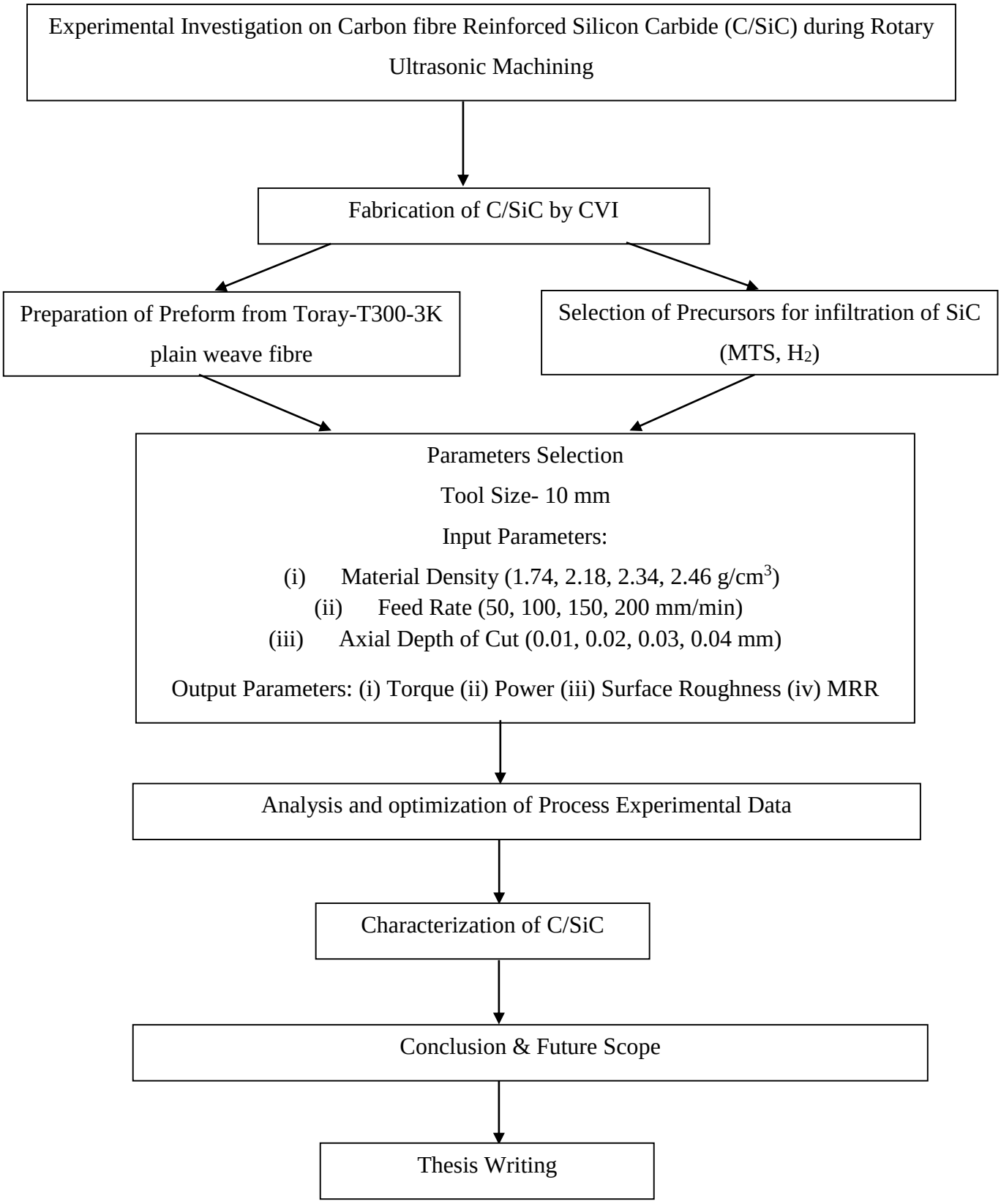
Experimental Investigation on Carbon fibre Reinforced Silicon Carbide (C/SiC) during Rotary Ultrasonic Machining
Fabrication of C/SiC by CVI
Preparation of Preform from Toray-T300-3K plain weave fibre
Selection of Precursors for infiltration of SiC (MTS, H2)
Parameters Selection
Tool Size- 10 mm
Input Parameters:
(i) Material Density (1.74, 2.18, 2.34, 2.46 g/cm3)
(ii) Feed Rate (50, 100, 150, 200 mm/min)
(iii) Axial Depth of Cut (0.01, 0.02, 0.03, 0.04 mm)
Output Parameters: (i) Torque (ii) Power (iii) Surface Roughness (iv) MRR
Analysis and optimization of Process Experimental Data
Characterization of C/SiC
Conclusion & Future Scope
Thesis Writing

Chapter-3

EXPERIMENTATION

This chapter discusses in detail the fabrication of C/SiC composite and experimental setup designed to carry out various surface milling tests on C/SiC. The machine and materials required for experimentations are:

The detailed description of the machine, machine tool, tool holder, work piece material and the measurement instruments used for this research work have been discussed in the following sections.

3.1 Fabrication of C/SiC:

C/SiC composite was fabricated by the chemical vapor infiltration technique. CVI reactor was present at the Ceramic Matrix Material Division (CMPD), Vikram Sarabhai Space Centre, Trivandrum. Complete fabrication can be classified in two steps.

In Step 1: the carbon fibre preform was prepared from the Toray-T300-3K plain weave fibre by using needling method. Firstly overlapping of 0° non-woven carbon cloth layer with 90° non-woven cloth layer was done. Then by needling method this lamina was joined with the carbon fibre bundle which was placed perpendicular to lamina. Squeezed rollers were used to remove the entrapped air between the preform. This process was repeated until desired thickness of 7 mm was achieved. At the end pyrolysing was done in the N_2 atmosphere by placing it inside the furnace at temperature of 1000 °C.

In second step, carbon preform was placed inside the CVI reactor. Methyltrichlorosilane (MTS) (CH_3SiCl_3) and Hydrogen (H_2) used as precursors for infiltration of SiC into the preform. MTS gas was passed from the flow chamber and mixed with hydrogen in the mixing chamber. This makes the SiC. The CVI reactor was heated at a slow rate of 3 °C/min. When the temperature of 1000 °C was obtained than temperature is stabilized for 10-20 min. When MTS/H_2 mixer entered the reactor, it infiltrate SiC in and around the carbon preform. Matrix wt % of SiC was increased by increasing the flow rate of MTS/ H_2 mixture.

Fig 3.1: The CVI System

3.1.1 Properties of Workpieces:

Properties of C/SiC workpieces are listed in table 3.1

Table 3. 1: Properties of workpieces

Sl. No.	Sample ID	Matrix Wt%	Density (g/cm^3) by Archimedes Method	Porosity (Vol. %) by Archimedes Method)
1	SCVI-1	55	1.74	1.7
2	SCVI-2	70	2.18	0.6
3	SCVI-3	79	2.34	2.3
4	SCVI-4	88	2.46	1.2

3.1.2 Mechanical Properties of C/SiC composite

Mechanical properties of C/SiC composite fabricated through CVI technique are listed in Table 3.2.

Table 3. 2: Mechanical properties of C/SiC fabricated through CVI

Tensile Strength	300-320 Mpa
Young's Modulus	90-100 GPa
Compression Strength	450-550 Mpa
Flexural Strength	450-500 Mpa

3.1.3 Properties of fibre:

Toray-T300-3K plain weave fibre was used while fabrication of C/SiC. Properties of the fibre are in Table 3.3.

Table 3. 3: Properties of fibre

Tensile Strength	4440.25 Mpa (644 ksi)
Young's Modulus	(32.0 msi)
Elongation	1.90 %
Density	1.80 g/cm^3

3.2 Description of Machining Setup

3.2.1 Rotary Ultrasonic Machine:

Whole experiments were carried out on CNC Ultrasonic 50 Sauer machine (Fig. 3.1). The maximum main drive power input to machine is 13 KW. The machine weight is 3920 Kg without tool and its maximum weight (with tool etc.) is 4320 Kg. The maximum length, width and height of machine is 2.21m, 1.92m, 2.15m respectively. It can be worked in both mode i.e. with or without ultrasonic.

Complete technical specifications are given in table 3.4. This is available at Advanced Manufacturing Facilities Division, Vikram Sarabhai Space Centre, Indian Space Research Organization (ISRO), Trivandrum.

Operations like drilling or face milling can be performed on it. It is mainly used for machining for advanced ceramics like zerodur, $MoSi_2$-SiC, Zirconium oxide, Silicon Carbide, Aluminum oxide etc.

Fig. 3. 2: Rotary Ultrasonic Machine

Table 3. 4: Specification of CNC Rotary ultrasonic machine

Control system	Sinumeric 840D
Interpolation	3-axis linear interpolation, B&C positioning axis
Travel	**Metric**
X-axis	500 mm
Y-axis	450 mm
Z-axis	400 mm
B-axis	+110°/-5°

C-axis	360°
Dimensions	**Metric**
Length	2205 mm
Width	1535 mm
Height	2424 mm
Weight	3920 Kg
Max. Weight (with tool etc.)	4320 Kg

Main Drive

Rotational speed (ultrasonic mode)	20-6000 rpm
Drive Power (100/40 % ED)	9/13 KW
Torque (40% DC)	83 Nm
Ultrasonic Frequency	17.5-29.5 KHz

Feed

Maximum Travers X/Y/Z	24 m/min
Maximum feed power X/Y/Z	4.8 KN
Rapid feed	5 m/min

Fixed Table

Pallet working Surface	700×500 mm
Max. load	500 kg

Tool

Maximum tool length	300 mm
Maximum tool diameter	80 mm
Tool clamping system	Hydraulically/ Mechanically

Electrical Data

Type of current	DC
Switching function	Closer
Output circuit	PNP
Operating voltage rating	24 V DC
Operating current rating	≤ 200 mA
Operating voltage	10-30 V DC
Switching frequency	≤ 1000 Hz
Voltage Drop	≤ 1.5 VI
No load current	≤10 mA

3.2.2 Tool Holder:

The tool holder holds and couples the tool with the transducer. It virtually imparts the energy and amplifies the amplitude of vibration. As the tool holder transfers the vibration so it must have adequate fatigue strength. The tool holder which was used with the Ø10 mm tool was UAS-(HSK-63S) - ER-20.

Fig. 3. 3: Tool holder (ER-20)

3.2.3 Tool:

C/SiC is brittle in nature so it is hard to perform milling with common cutting tool. As due to anisotropy and fabrication structure of PCD twist drill, the carbon fibre are easy to tear during machining if drilling force is high. So diamond milling cutter of Ø10 mm of outer diameter and Ø8 mm of inner diameter with grain size of D64H was used for the machining. Tool ID was Schott-1800312.18

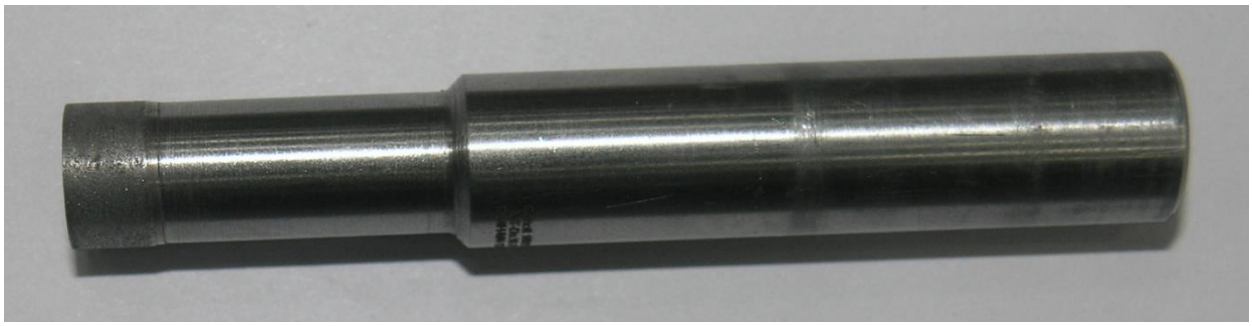

Fig. 3. 4: Diamond Tool (Ø10)

3.3 Design of Experiment:

Design of experiment is an efficient procedure to determine the relationship between factors which affect the process and its output. It is applied to analyze the data to yield valid and objective conclusions. For a given set of factors, a full factorial design can identify all the possible combination. But Taguchi provides a method which reduces the no. of experiments and provides the effect of all the factors.

3.3.1 Taguchi Method:

Dr. Genichi Taguchi of Nippon Telephones and Telegraph Company, Japan has developed a method of conducting the design of experiments. This method uses a special set of arrays known as orthogonal array. Experiments conducted by using orthogonal array provide much reduced “variance” for the experiment with “optimum settings” of control parameters.

3.3.2 Orthogonal Array:

Orthogonal Arrays are those efficient test plans that have been developed by Taguchi. These are basically a family of Fractional Factorial Experiments (FFE). The

unique feature of the orthogonal Array is that it allows the degrees of freedom of error to be traded for factor degrees of freedom and provide the particular test combinations that accommodate the approach.

The real power of Orthogonal Array is its ability to evaluate several factors in a minimum number of tests. Within the few trials, it provides the orthogonality among all the factors. This is considered an efficient experiment since much experiment is obtained from a fewer trials.

If all the columns are assigned a factor, then it is called saturated design. Assigning factors to a saturated design is not much difficult. However, unsaturated FFE may increase the complexity of the design.

3.3.3 Assumptions of the Taguchi method

Since the effect of each factor may be linear, quadratic or of higher order, but the taguchi method assumes that interactions of individual factor i.e. their cross product is not available. This implies that the effect of one independent variable does not depend on any other independent parameter with their different levels and vice versa. If in any case, this assumption is despoiled then it alters the additivity of main effects and interaction occur between the variables.

3.3.4 Procedure of Experimental Design:

The whole procedure of Taguchi method contains following steps-

1) State the objective.
2) Choose response.
3) Choose the factors and/ or interaction to be evaluated.
4) Select the number of levels and corresponding values for the factors.
5) Select the appropriate orthogonal array.
6) Assign the factors and interactions to the columns in orthogonal array.
7) Choose an experimental plan.
8) Perform the experiment.
9) Analyze the results.

3.3.5 Analysis of Results:

Signal to Noise Ratio

S/N ratio is used as an objective function for parameter optimization. Control factors can be adjusted easily and their values are define by us. Quality characteristic is mainly depend on these control factors. Noise factors like temperature, humidity, weather etc. are difficult or impossible to control. The ratio of the mean (signal) with the standard deviation (noise) is termed as the S/N ratio. For analysis purpose, taguchi gave three type of S/N ratio which described below-

(1) SMALLER-THE-BETTER:

$n = -10 \log_{10}$ (mean sum of square of experimental data)

This is mainly selected for all unwanted characteristics whom we want minimum like defects etc. Also, it is used to find the difference between the standard or ideal value of any data to it's measured value (like in case of measuring surface roughness of any material, if required value is 0.02 μm and experimental value are in some finite rate) then the difference between the standard data and experimental data is require to minimum. Then formula for calculating S/N ratio is,

$n = -10 \log_{10}$ [mean sum of square of (experimental data – ideal data)]

(2) THE-LARGER-THE-BETTER:

$n = -10 \log_{10}$ [mean sum of squares of reciprocal of experimental data]

This is require for maximizing some data. This is generally used for desired results, as they require to be maximum as possible like material removal rate.

(3) THE-NOMINAL-THE-BEST:

This case is used for achieving a required value. It was used when a certain value is desirable and neither higher nor small value from that value is require.

$$n = \frac{mean\ sum\ of\ squre\ of\ data}{variance\ of\ data}$$

3.4-Experimental Details:

3.4.1-Material Preparation:

C/SiC materials are initially not of uniform thickness. Facing was done on C/SiC specimens by using Rotary ultrasonic milling with the cutter of 60 mm diameter with grit size D151H.

After facing specimens are obtained of following dimensions,

Table 3. 5: Dimensions of Workpieces

S No.	Material Density	Size
1	1.74 g/cm^3	90×90×5 mm^3
2	2.18 g/cm^3	60×60×5 & 55×90×5 mm
3	2.34 g/cm^3	90×90×5 mm^3
4	2.46 g/cm^3	90×90×5 mm^3

Fig. 3. 5: Initial image of a specimen

3.4.2-Clamping Methodology:

For chatter free operations, proper fixturing is required. Fixture was primarily use to create a secure mounting point for a workpiece. Since material surface is uneven. So specimen are placed on plane metallic plate by pasting with petroleum wax on the surface of material. The wax was melt on the surface of fixture before placing the workpiece. Then these plates are clamped on the RUM's table. After the milling process, the fixture was heated using a heater so that the wax melt again and the workpiece was released from the fixture. The workpiece surface and fixture surface was cleaned of the wax by wiping the surfaces with acetone.

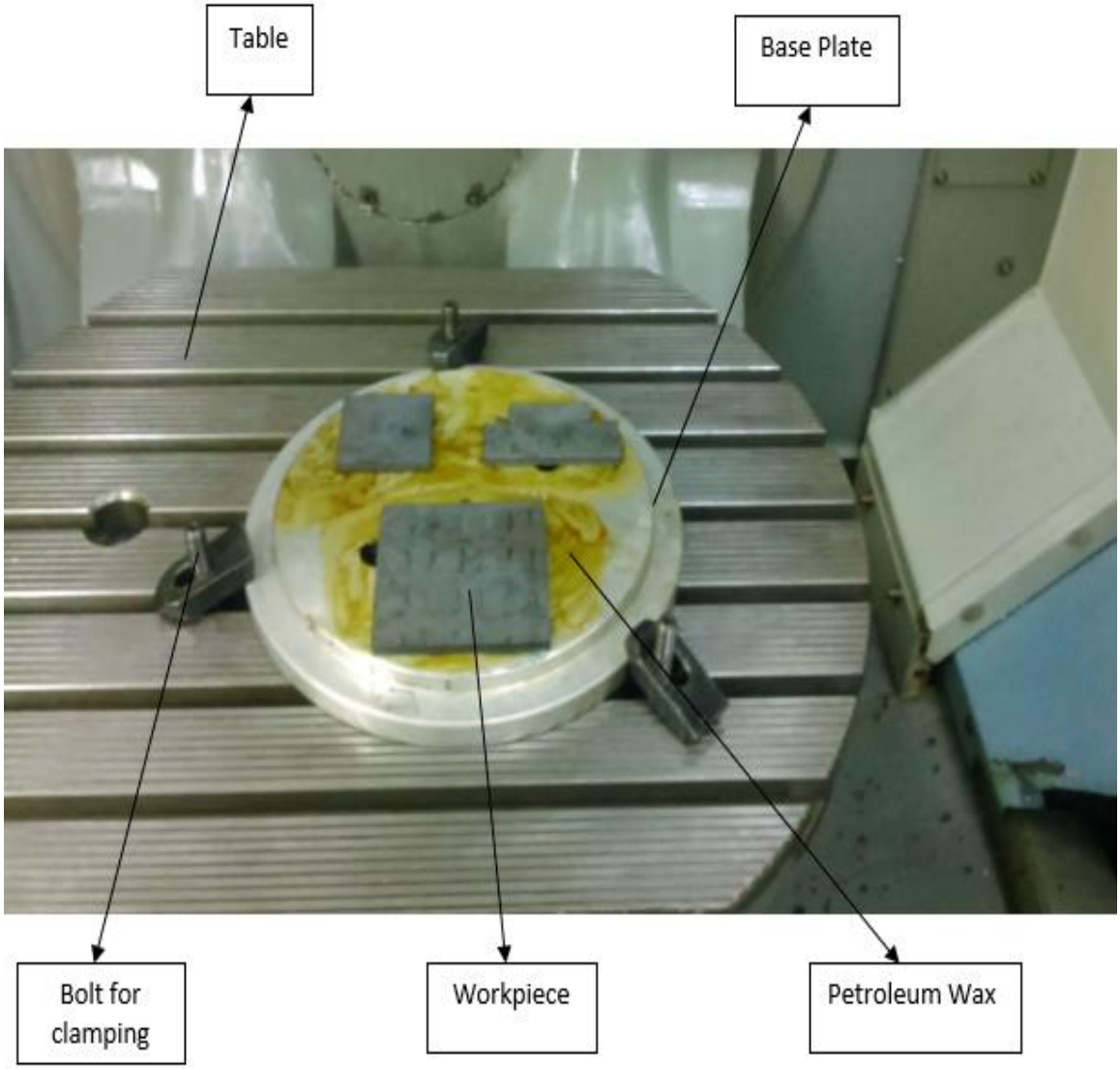

Fig. 3. 6: Clamping of Workpiece

3.5-Rotary Ultrasonic Milling of C/SiC:

The experimentation was carried out in two phases as given below:

1) The initial phase involved the screening experiments to identify the important milling parameters for the study and to eliminate the unwanted parameters from the study.
2) The second phase involved carrying out actual milling operation using the milling parameters identified for the study.

3.5.1-Screening Experiment:

The screening experiments were carried out by varying each process parameter over a range of values and then studying their influence on the face milling process.

The process parameters involved the various machining parameters and also the various material parameters. The machining parameters that were varied were cutting speed, axial depth of cut, feed rate, vibration frequency, amplitude. Coolant pressure.

The material parameter that varied were the material density and thickness of material.

3.5.2 Selection of parameters:

From the performed screening experiments, machining constraints and working constraints, identified milling parameters were-

- Material Density
- Feed Rate (F)
- Axial Depth of cut (D_a)

These parameters were selected for further study. While other parameters such as Spindle Speed, Amplitude, frequency, Radial Depth of cut were keeping constant. Coolant was provided by both way i.e. around the tool and through the tool. There are valid theoretical relations that connect the parameters that were selected for the study and the parameters that were eliminated based on the screening phase.

The levels of each parameter were finalized based on the screening experiments carried-out initially and the theoretical calculations based on the relations available.

The lists of factors studied with their levels are given in Table 3.6.

Table 3. 6: Control variables and their levels

S. No.	Factor	Level 1	Level-2	Level-3	Level-4
1	Material Density (g/cm^3)	1.74	2.18	2.34	2.46
2	Feed rate (mm/min)	50	100	150	200
3	Axial Depth of Cut (mm)	0.01	0.02	0.03	0.04

The values of constant parameters are listed in Table 3.7 below:

Table 3. 7: Constant parameters during RUM of C/SiC

Spindle speed	6000 rpm
Amplitude	50 %
Frequency	27.5-28 KHz
Radial Depth of Cut	4 mm

The effect of the process parameters were measured on the following performance characteristics.

- Torque
- Change in Surface Roughness
- MRR

3.5.3 Calculation of Total Degree of Freedom:

The degree of freedom of a four level parameter is three (number of level-1). Hence total degree of freedom is 9

Table 3. 8: Degree of freedom as per level

Input Parameters	Unit	DOF
Material Density (A)	g/cm^3	3
Feed rate (B)	mm/min	3
Depth of cut (C)	Mm	3
Error		6
	Total	15

3.5.4 Selection of appropriate orthogonal Array:

Out of the standard orthogonal array available in Taguchi design, L16 orthogonal array has fifteen degree of freedom and it can lodged four levels of three parameters, so it has been chosen for the experimentation. In addition, there is no loss in the orthogonality of array if more than one column does not used. Thus sixteen experiments are required to be performed. Taguchi also recommends that effect of uncontrolled factors can be minimizes by repeating each set of experiment minimum three times. Therefore, each set of sixteen experiments was repeated three times. L-16 array was presented in Table-3.9

Table 3. 9: L16 array in Taguchi

Experiment No.	A	B	C
1	1	1	1
2	1	2	2
3	1	3	3
4	1	4	4
5	2	1	2
6	2	2	1
7	2	3	4
8	2	4	3
9	3	1	3
10	3	2	4
11	3	3	1

12	3	4	2
13	4	1	4
14	4	2	3
15	4	3	2
16	4	4	1

3.5.5 Actual Milling Process:

Rotary ultrasonic face milling of C/SiC was carried out as per the L16 table 3.4. A total of 16 experiments were conducted (Fig 3.8, Fig 3.9, Fig 3.10, Fig. 3.11). Parameters for each experiment are listed in Table 3.10.

Table 3.10: Taguchi L-16 array for RUM of C/SiC

Experiment No.	Material Density (g/cm^3)	Feed Rate (mm/min)	Axial Depth od Cut (mm)
1	1.74	50	0.01
2	1.74	100	0.02
3	1.74	150	0.03
4	1.74	200	0.04
5	2.18	50	0.02
6	2.18	100	0.01
7	2.18	150	0.04
8	2.18	200	0.03
9	2.34	50	0.03
10	2.34	100	0.04
11	2.34	150	0.01

12	2.34	200	0.02
13	2.46	50	0.04
14	2.46	100	0.03
15	2.46	150	0.02
16	2.46	200	0.01

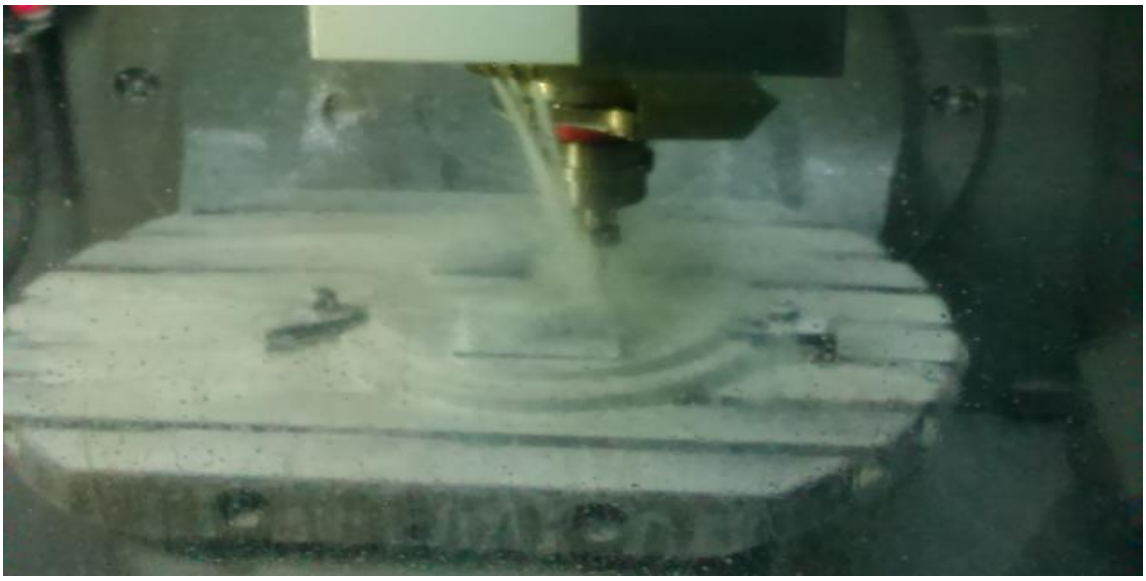

Fig. 3. 7: Rotary Ultrasonic Milling of Workpiece

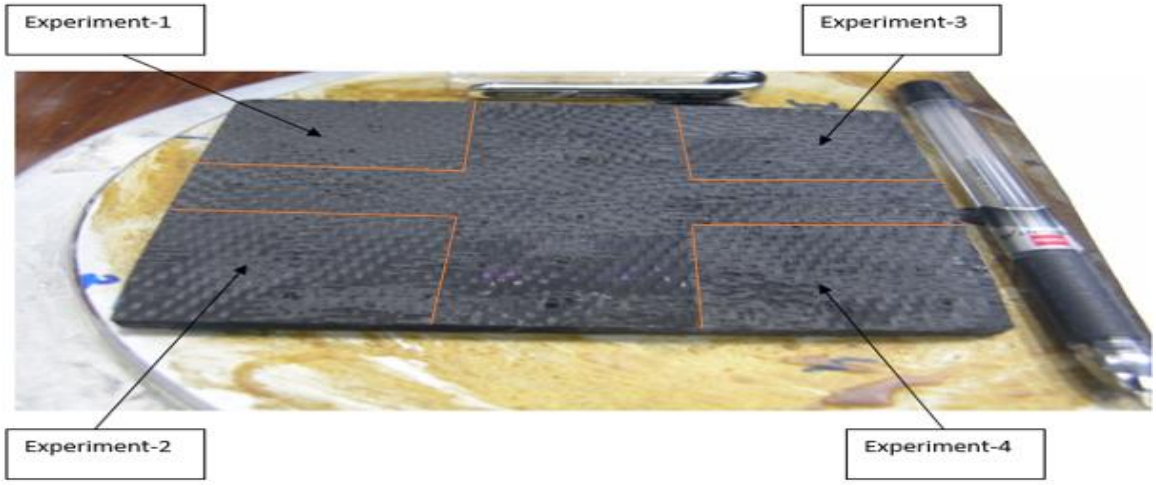

Fig. 3. 8: C/SiC of material density 1.74 g/cm^3 after RUM

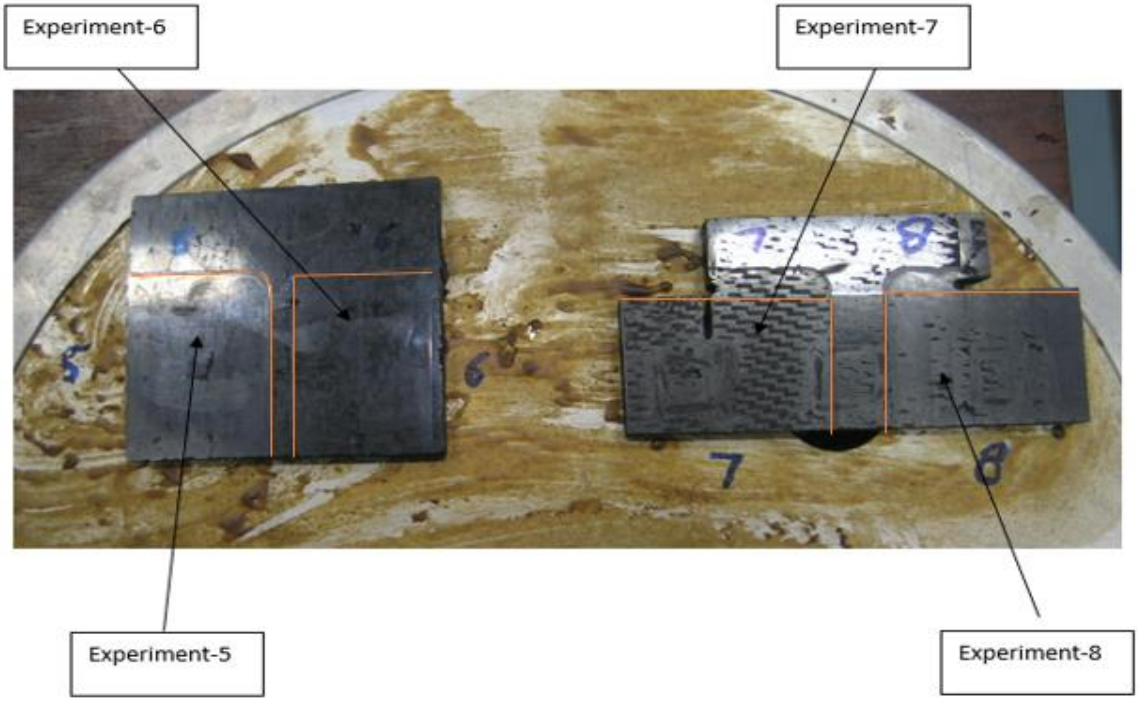

Fig. 3. 9: C/SiC of material density 2.18 g/cm^3 after RUM

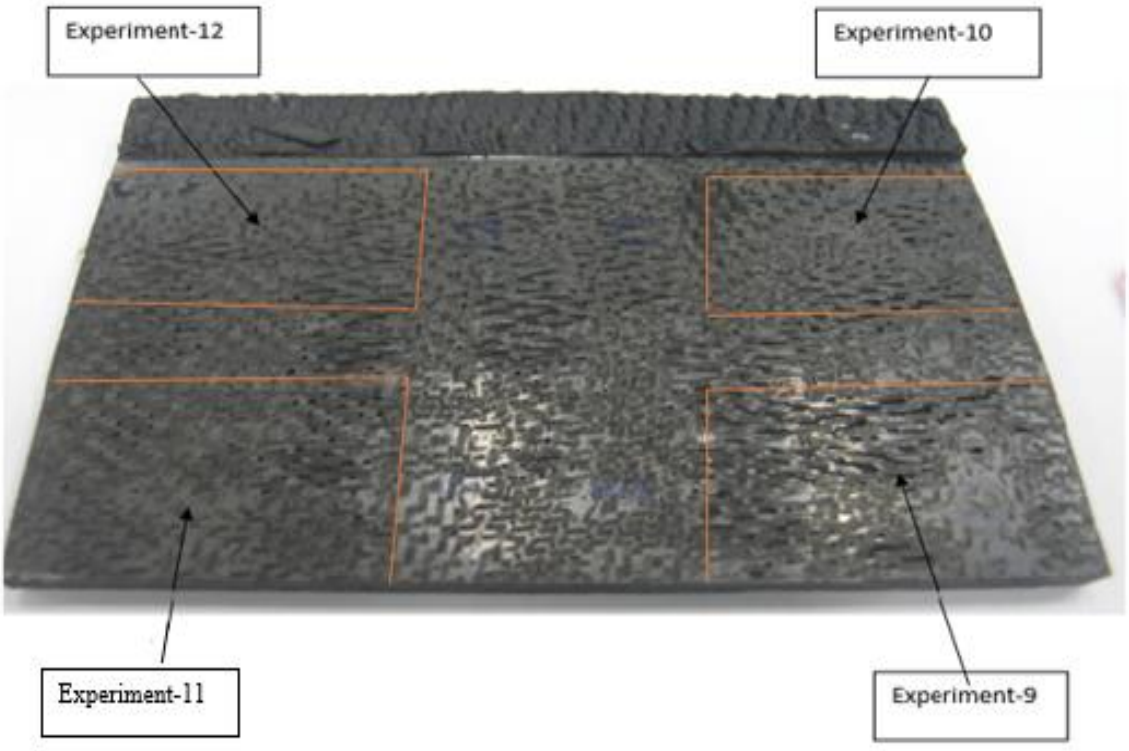

Fig. 3. 10: C/SiC of density 2.34 g/cm^3 after RUM

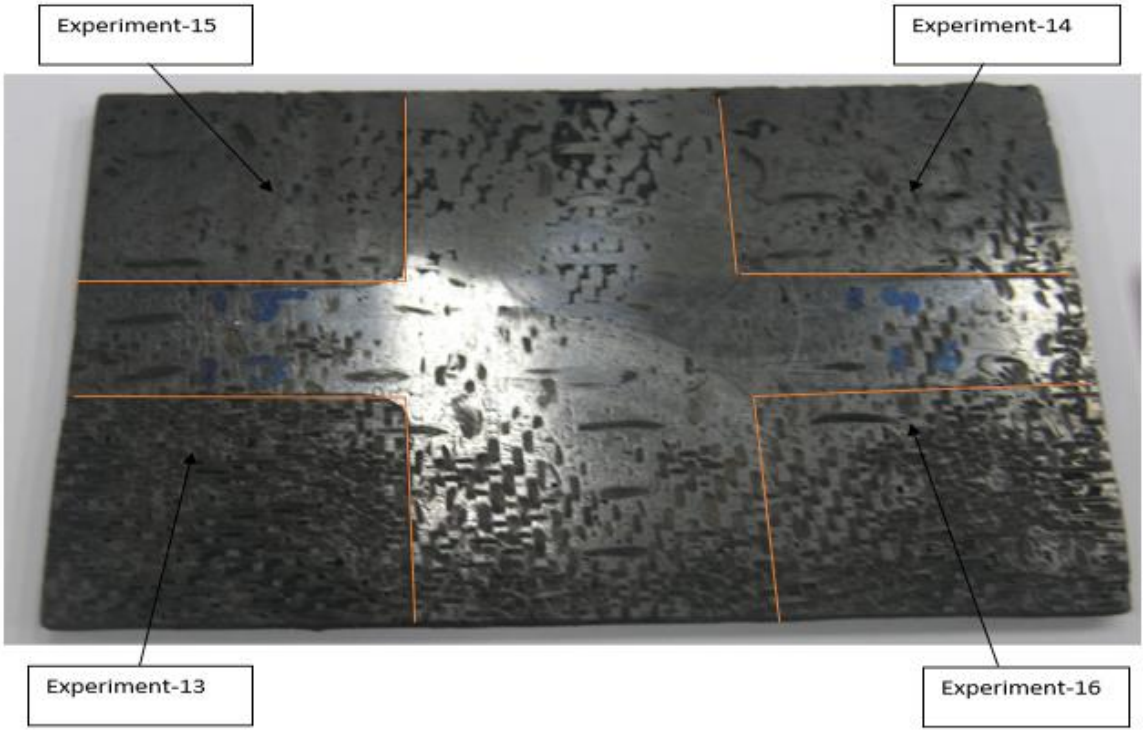

Fig. 3. 11: C/SiC of density 2.46 g/cm^3 after RUM

3.5.6 Measurement of Material removal rate (MRR):

MRR was measured manually by calculating the volume of material removal and time taken by the machine for doing the face milling. This time was measured by the stop watch (least count: 0.01 min). Formula used for calculating the MRRwas-

$$MRR = \frac{Volume\ of\ Material\ Reoved}{Time\ taken\ for\ Machining}$$

Where:

Volume = (length × width × thickness), mm^3

Time in minute

3.5.7 Measurement of Torque:

Rotary USM machine, Ultrasonic 50 Sauer which was used for experimentation provides direct values of torque exerted on the tool. These values was display on the Sinumeric Siemens 840D controller's screen.

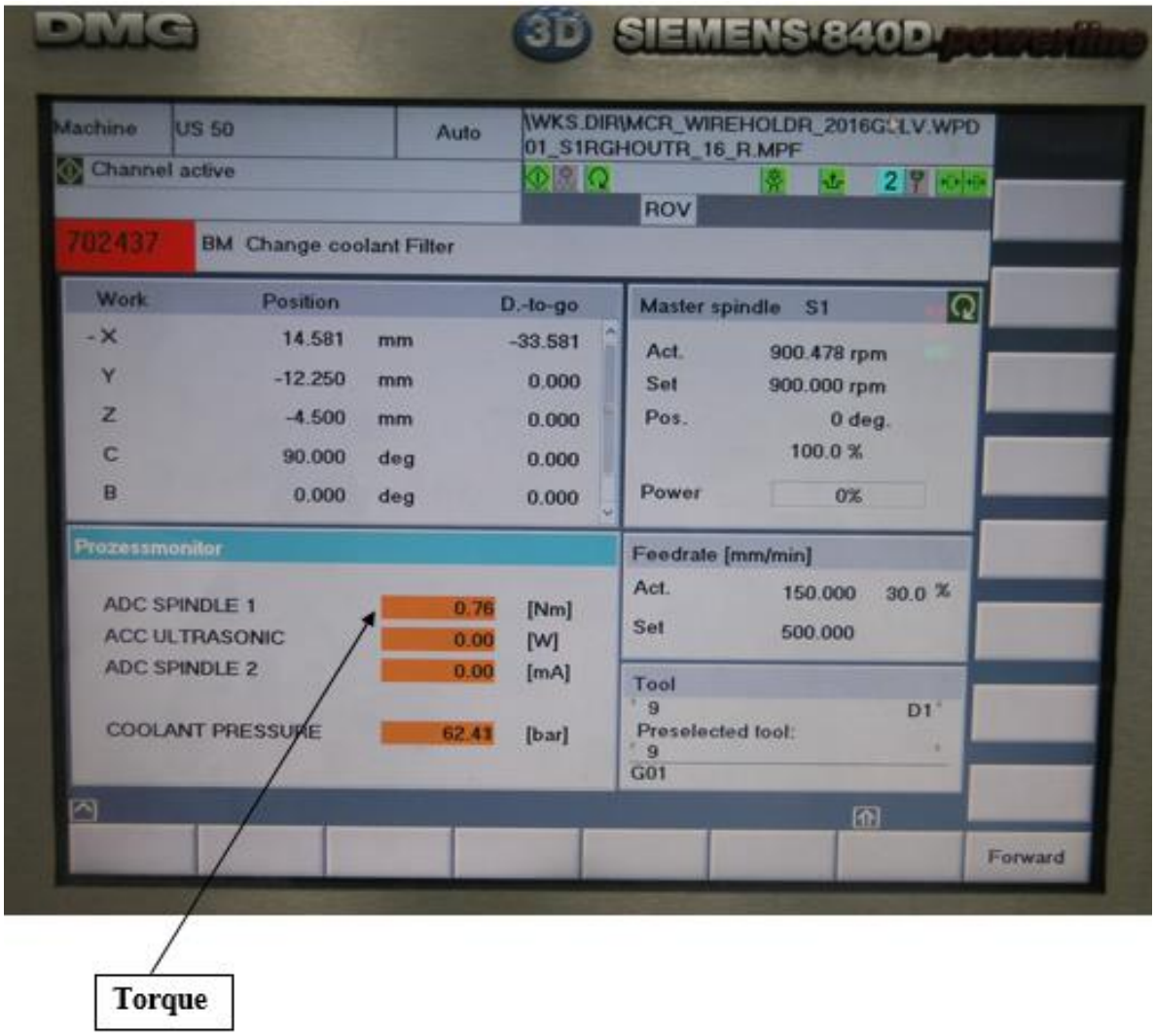

Fig. 3. 12: Sinumeric 840D controller's display

3.5.8 Change in Surface Roughness Measurement:

As all the four work piece have different initial surface roughness. So for checking the machining effect on surface finish of C/SiC, change in surface roughness was calculated. Surface roughness before and after of all experiments were measured on the talysurf which was present at 'QIT division, Vikram Sarabhai Space Center, ISRO Trivandrum'. For measuring the surface roughness, stylus which is attached in the talysurf was slides on the workpieces. The stylus have a 2µm diamond tip. This talysurf was attached to a computer which have 'Taylor-Hobson ultra-software', when stylus slides on the workpiece, software shows the values.

Fig. 3. 13: Setup of Talysurf

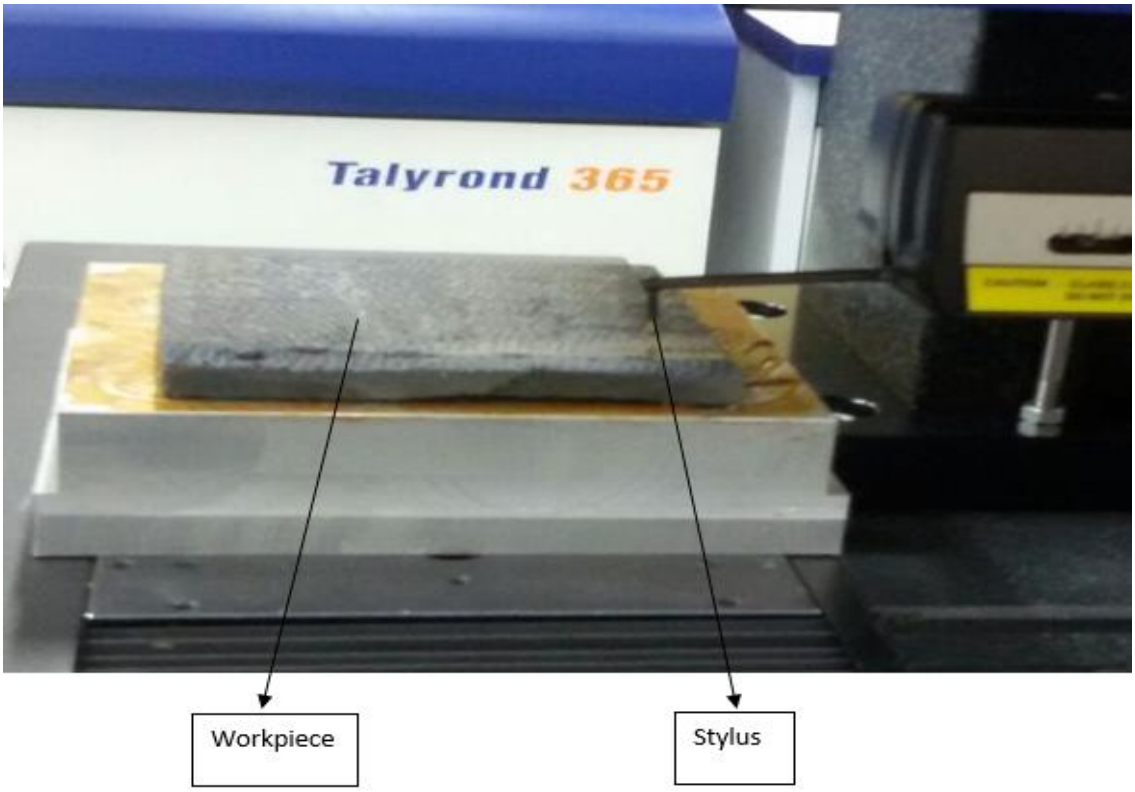

Fig 3.14: close view of Stylus on workpiece

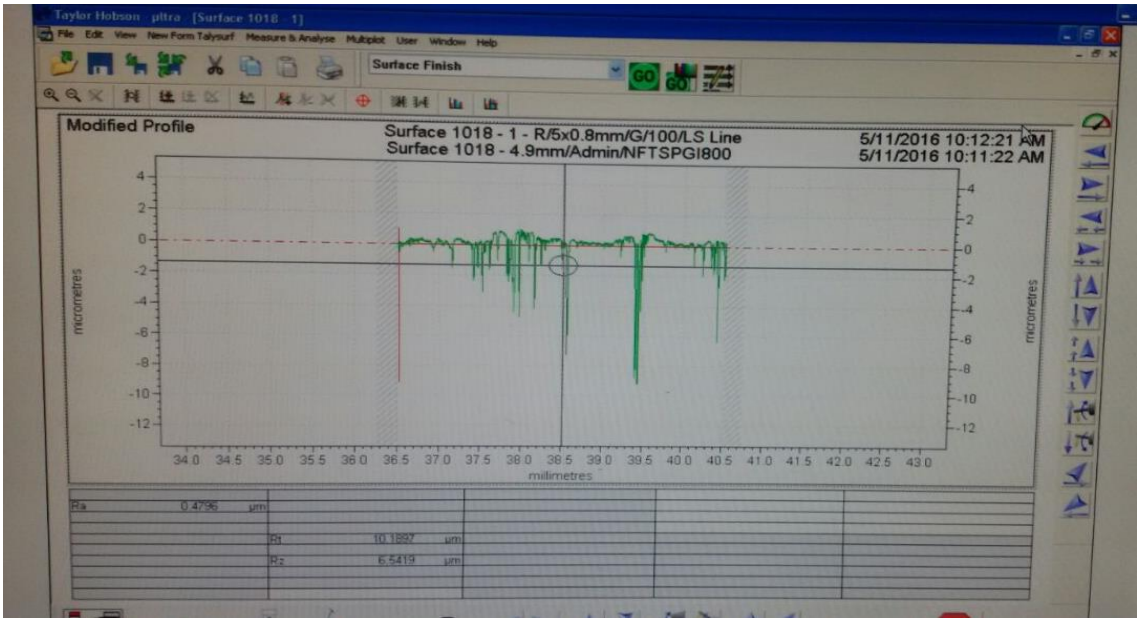

Fig 3.15: Graph for surface roughness

3.6 Analysis of Variance (ANOVA):

The steps carried out in analysis of variance are listed as under:

1. **Total of all results (T)**

$$T = \sum_{i=1}^{n}\sum_{j=1}^{R} y_{ij} \ ;$$

n = Total number of trials = 16

R = Total number of repetitions = 3

2. **Correction factor (C.F.)**

C.F. = T^2/N

N = Total number of experiments = 16*3 = 48

3. **Total sum of squares (SS_T)**

$$SS_T = \sum_{i=1}^{n}\sum_{j=1}^{R} y_{ij}^2 - C.F.$$

4. **Sum of squares due to a parameter (SS)**

$$SS_A = \left[{A(1)^2}/{N_{A_1}} + {A(2)^2}/{N_{A_2}} + {A(3)^2}/{N_{A_3}} \right] - C.F.$$

Where, $N_{A1,}$ $N_{A2,}$ NA_3 are number of trails with parameter A at level 1, 2 and 3 respectively.

The sum of squares SS_B and $SS_{C,}$ are calculated in the similar way.

5. Error sum of squares (SS_e)

$SS_e = SS_T – (SS_A + SS_B + SS_C)$

The symbol 'e' stands for error term.

6. Mean square of variance (V)

V_A = Variance due to parameter A = SS_A / f_A

$V_B = SS_B / f_B$, $V_C = SS_C / f_C$

V_e = Variance due to error = SS_e / f_e

7. Percentage contribution (P)

P_A = % contribution of parameter A towards mean of the response

$= (SS_A/ SS_T) * 100$

Similarly, $P_B = (SS_B/ SS_T) * 100$, $P_C = (SS_C/ SS_T) * 100$ and $Pe = (SS_e/ SS_T) * 100$

8. F- Ratios

$F_A = V_A / V_e$, $F_B = V_B / V_e$, $F_C = V_C / V_e$

Chapter-4

ANALYSIS AND DISCUSSIONS OF RESULTS

This chapter focuses on the experimental results, analysis and discussion of main experiments of rotary ultrasonic milling of C/SiC.

4.1 Results:

The values obtained after every experiment for various output parameters have been recorded in various tables i.e. Table-4.1, Table-4.2 and Table-4.3

Table 4. 1: Results table for Torque (Ƭ)

Exp. No.	Material Density (g/cm^3)	Feed rate (mm/min)	D_a (mm/min)	$Ƭ_1$ (Nm)	$Ƭ_2$ (Nm)	$Ƭ_3$ (Nm)	Avg. Torque (Ƭ) (Nm)	SN ratio for Ƭ
1	1.74	50	0.01	0.13	0.11	0.12	0.12	18.4164
2	1.74	100	0.02	0.18	0.21	0.18	0.19	14.4249
3	1.74	150	0.03	0.27	0.29	0.28	0.28	11.0568
4	1.74	200	0.04	0.32	0.31	0.33	0.32	9.8970
5	2.18	50	0.02	0.15	0.16	0.17	0.16	15.9176
6	2.18	100	0.01	0.19	0.17	0.18	0.18	14.8945
7	2.18	150	0.04	0.33	0.31	0.29	0.31	10.1728
8	2.18	200	0.03	0.32	0.30	0.31	0.31	10.1728
9	2.34	50	0.03	0.21	0.25	0.23	0.23	12.7654
10	2.34	100	0.04	0.33	0.31	0.32	0.32	9.8970
11	2.34	150	0.01	0.22	0.21	0.20	0.21	13.5556
12	2.34	200	0.02	0.27	0.25	0.26	0.26	11.7005
13	2.46	50	0.04	0.26	0.28	0.30	0.28	11.0568
14	2.46	100	0.03	0.33	0.37	0.35	0.35	9.1186
15	2.46	150	0.02	0.30	0.29	0.28	0.29	10.7520
16	2.46	200	0.01	0.26	0.28	0.24	0.26	11.7005

Table 4. 2: Results Table for MRR

Exp. No.	Material Density (g/cm^3)	Feed rate (mm/ min)	D_a (mm)	MRR-1 (mm^3/min)	MRR-2 (mm^3/min)	MRR-3 (mm^3/min)	Avg. MRR (mm^3/min)	SN ratio for MRR
1	1.74	50	0.01	1.98	2.01	2.01	2.00	6.0206
2	1.74	100	0.02	7.92	7.896	7.884	7.90	17.9525
3	1.74	150	0.03	17.9764	17.9806	17.983	17.98	25.0958
4	1.74	200	0.04	31.941	31.822	32.027	31.93	30.0840
5	2.18	50	0.02	3.968	3.917	4.025	3.97	11.9758
6	2.18	100	0.01	3.961	3.964	3.925	3.95	11.9319
7	2.18	150	0.04	23.891	23.907	23.902	23.90	27.5680
8	2.18	200	0.03	23.915	23.931	23.914	23.92	27.5752
9	2.34	50	0.03	6.1	6.03	6.02	6.05	15.6351
10	2.34	100	0.04	16.02	15.99	15.93	15.98	24.0715
11	2.34	150	0.01	5.974	5.967	5.969	5.97	15.5195
12	2.34	200	0.02	16.01	16.05	16.03	16.03	24.0987
13	2.46	50	0.04	7.985	8.014	8.013	8.01	18.0727
14	2.46	100	0.03	12	11.98	11.96	11.98	21.5691
15	2.46	150	0.02	11.964	11.949	11.937	11.95	21.5474
16	2.46	200	0.01	7.948	7.961	7.941	7.95	18.0073

Table 4. 3: Results table for Change in Surface Roughness (Ra)

Exp. No.	Material Density (g/cm^3)	Feed rate (mm/min)	D_a (mm)	Initial Ra	Change Ra1 (µm)	Change Ra2 (µm)	Change Ra3 (µm)	Average Ra (µm)	SN ratio for Ra
1	1.74	50	0.01	14.89	6.11	6.05	6.08	6.08	15.6781
2	1.74	100	0.02	14.89	5.56	5.61	5.57	5.58	14.9327
3	1.74	150	0.03	14.89	5.01	4.96	4.97	4.98	13.9446
4	1.74	200	0.04	14.89	4.48	4.52	4.47	4.49	13.0449
5	2.18	50	0.02	6.43	3.80	3.84	3.82	3.82	11.6413
6	2.18	100	0.01	6.43	3.42	3.46	3.47	3.45	10.7564
7	2.18	150	0.04	6.43	3.01	3.03	3.02	3.02	9.6001
8	2.18	200	0.03	6.43	2.88	2.83	2.87	2.86	9.1273
9	2.34	50	0.03	5.76	2.69	2.65	2.64	2.66	8.4976
10	2.34	100	0.04	5.76	2.29	2.28	2.30	2.29	7.1967
11	2.34	150	0.01	5.76	2.28	2.33	2.32	2.31	7.2722
12	2.34	200	0.02	5.76	2.17	2.13	2.12	2.14	6.6083
13	2.46	50	0.04	2.04	.88	.95	.93	0.92	-0.7242
14	2.46	100	0.03	2.04	0.84	0.86	0.88	0.86	-1.3100
15	2.46	150	0.02	2.04	0.80	0.79	0.84	0.81	-1.8303
16	2.46	200	0.01	2.04	0.78	0.75	0.78	0.77	-2.2702

4.2 Effect of parameters on Torque:

Fig 4.1, Fig 4.2 showing the variation of Torque is linear with all the process parameters. Mean effect graph shows that torque is increasing with the increase in material density, feed rate and axial depth of cut.

Torque is increasing with the depth of cut as the load on the tool increases with increase of penetration of tool. This will increase the cutting force required for milling which finally increases the torque.

With the increase in the material density of C/SiC composite, the concentration of silicon carbide in C/SiC increases. It increases the hardness of composite which makes the machining difficult, so torque increases.

Torque increases with increase in feed rate as the contact between tool and workpiece increases.

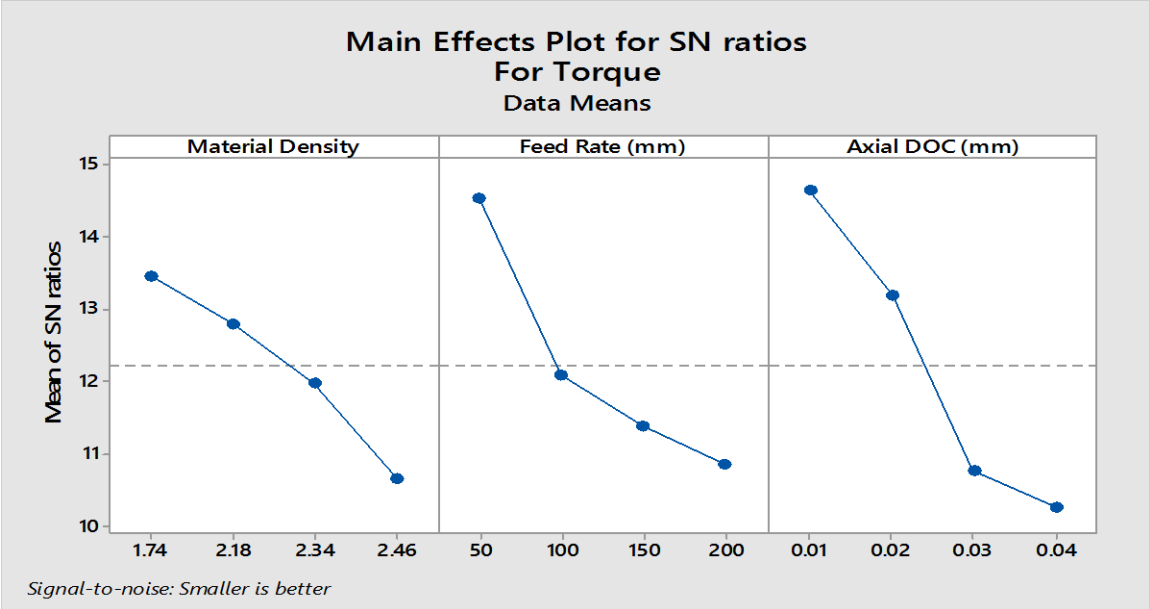

Fig. 4. 1: SN ratio graph for torque (T)

4.2.1 Selection of Optimal Levels:

Table 4.4 & 4.5 are the response table for S/N ratio and mean for the torque. They shows the rank of the parameters. Torque in RUM process is largely depends on axial depth of cut than feed rate and minimum on material density in these selected parameters.

The average values of S/N data at different levels of the parameters are plotted along with average values of the torque in Fig. 4.1 for C/SiC composite. The effect of axial depth of cut and feed rate is more predominant than the material density. Anova table for S/N ratio for torque (Table 4.6) shows that al the parameters have significant effect on the torque generated during RUM of C/SiC composite. Axial depth of cut affects most i.e. 50.85 % and material density least with 17.27 %. Level 1 of material density, feed rate and axial depth of cut corresponds to the minimum mean response and maximum S/N ratio for C/SiC.

Hence it is clear that the minimum torque was found on material of material density 1.74 g/cm^3 at 50 mm/min feed rate and 0.01 mm axial depth of cut.

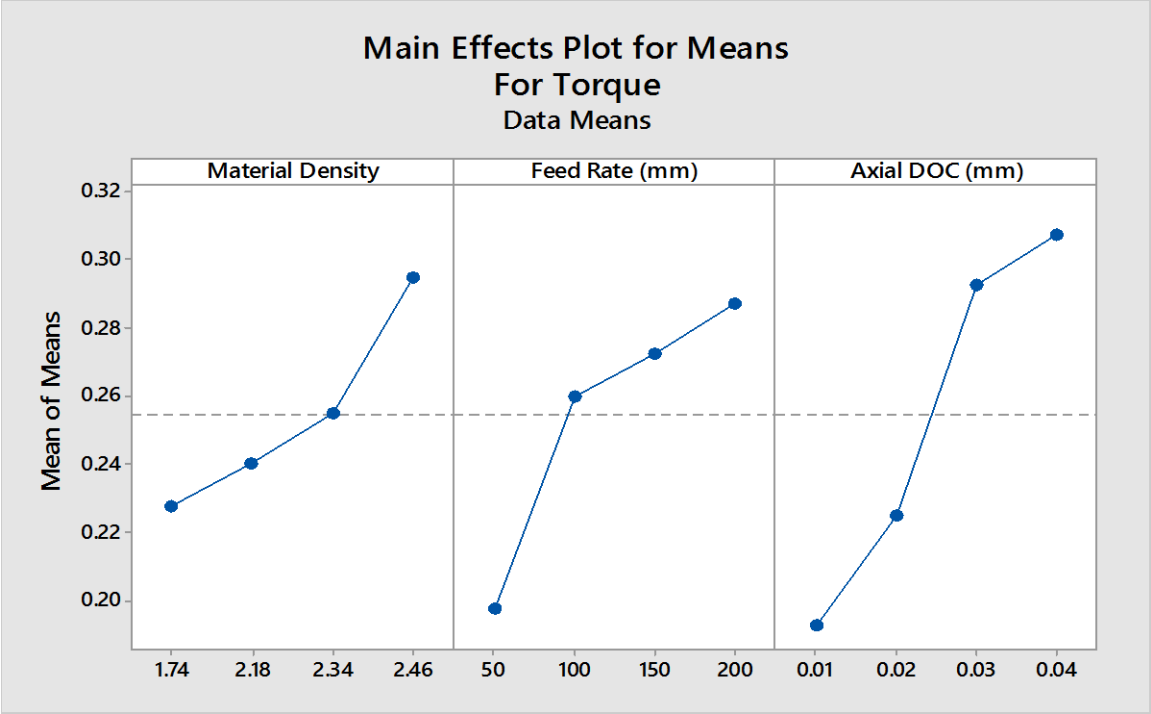

Fig. 4. 2: Mean effect graph for Torque (Ƭ)

Table 4. 4: Response Table for S/N ratio (Torque)

Level	Material Density	Feed Rate	Axial DOC
1	13.45	14.54	14.64
2	12.79	12.08	13.20

3	11.98	11.38	10.78
4	10.66	10.87	10.26
Delta	2.79	3.67	4.39
Rank	3	2	1

Table 4. 5: Response Table for means (Torque)

Level	Material Density	Feed Rate	Da
1	0.2275	0.1975	0.1925
2	0.2400	0.2600	0.2250
3	0.2550	0.2725	0.2925
4	0.2950	0.2875	0.3075
Delta	0.0675	0.0900	0.1150
Rank	3	2	1

Table 4. 6: ANOVA for S/N Ratio of Torque (Ţ)

Source	DOF	SS	Mean Sum of Square	F	P	% Contribution
Material Density	3	17.339	5.7798	120.29	0.000	17.27
Feed Rate	3	31.695	10.5649	219.89	0.000	31.58
Da	3	51.035	17.0117	354.06	0.000	50.85
Residual Error	6	0.288	0.0480			
Total	15	100.357				

4.3 Effect of parameters on Material Removal Rate

Table 4.2 shows that MRR in rotary ultrasonic milling of C/SiC composite have been found to be correlated and dependent upon the input parameters. The average values of each of the raw data and S/N ratio at different levels are considered and plotted in Fig. 4.3, 4.4 respectively.

It is clear from the mean effect graph (Fig 4.4) that MRR was more with material of minimum SiC density (1.74 g/cm^3). This can be explained on the basis of hardness of composite which is minimum for the material with lower C/SiC density. MRR plot shows that it increases with increase in feed rate and depth of cut. This is happening due to the increase in material contact with the tool.

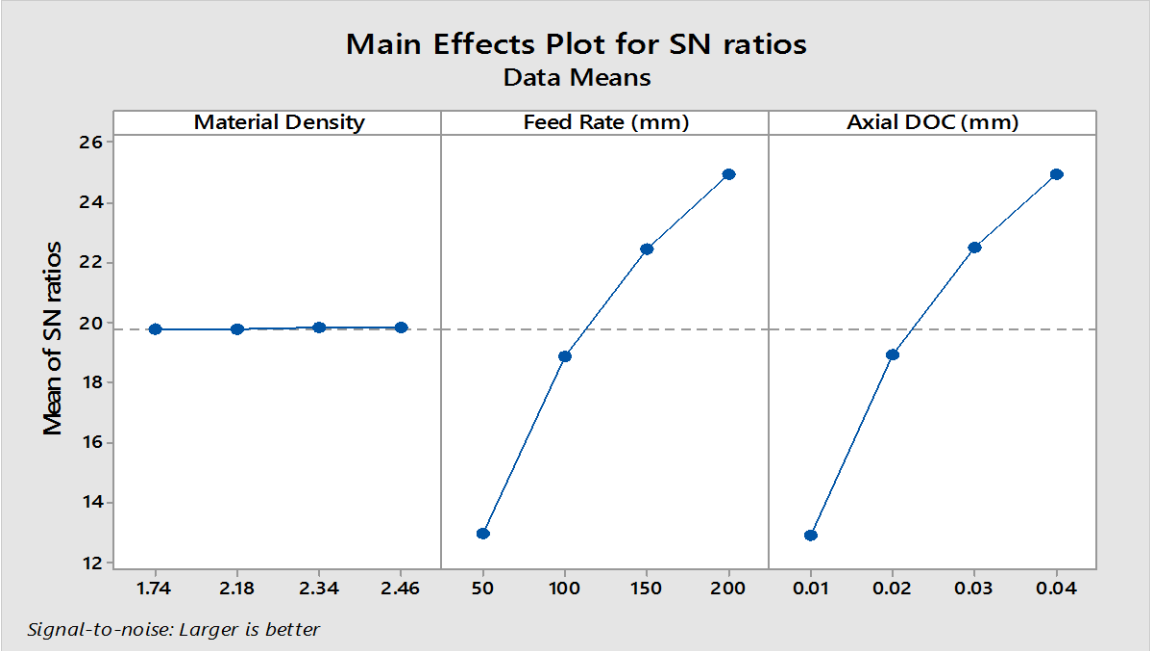

Fig 4.3: SN ratio graph for MRR

4.3.1 Selection of Optimal Levels:

Table 4.7 & 4.8 are the response table for S/N ratio and mean for the material removal rate. They shows the rank of the parameters. MRR in RUM process is largely depends on axial depth of cut than feed rate and minimum on material density in these selected parameters.

The average value of S/N ratio are plotted in Fig. 4.3 for C/SiC composite. A visual examination clearly indicates that material removal rate is maximum at first level of material density, fourth level of feed rate and axial depth of cut.

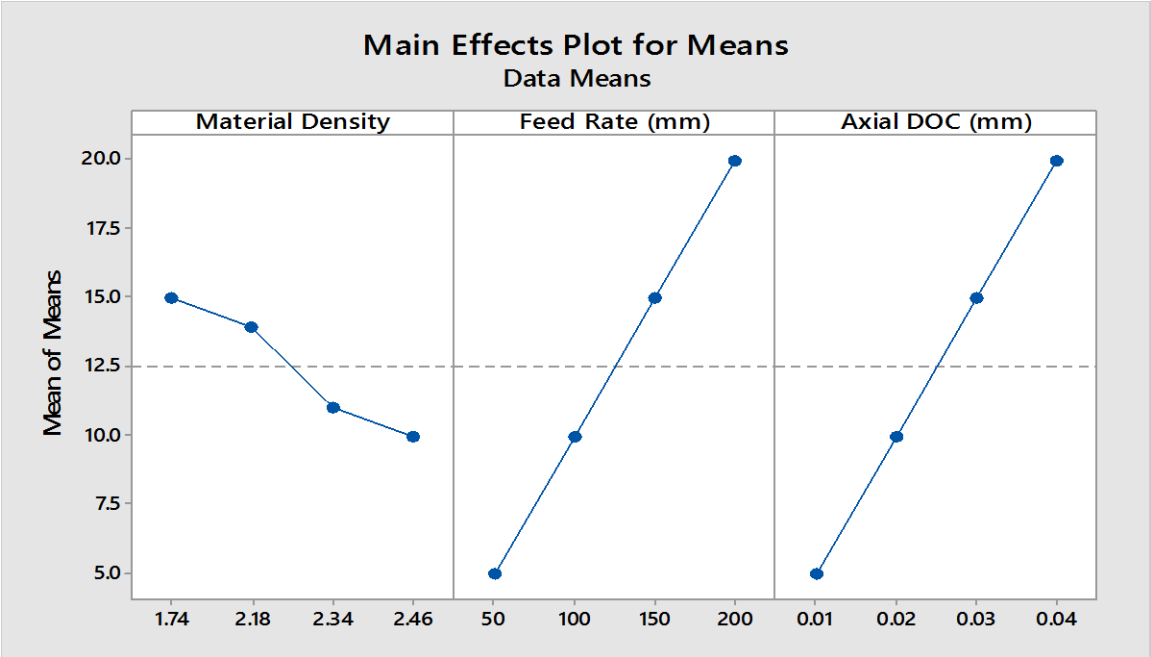

Fig 4.4: Mean effect graph for MRR

ANOVA table for S/N ratio (Table 4.9) of MRR clearly shows that MRR is highly dependent on axial depth of cut and feed rate. Effect of material density is negligible on to the MRR. The percentage contribution of axial depth of cut is maximum i.e. 50.31 % and for feed rate is 49.69 %.

Hence maximum MRR was found on material of 1.74 g/cm^3 material density at feed rate of 200mm/min and axial depth of cut of 0.04 mm.

Table 4. 7: Response Table for S/N ratio of (MRR)

Level	Material Density	Feed Rate	Axial DOC
1	19.79	12.93	12.87
2	19.76	18.88	18.89
3	19.83	22.43	22.47

4	19.80	24.94	24.95
Delta	0.07	12.02	12.08
Rank	3	2	1

Table 4. 8: Response Table for means of MRR

Level	Material Density	Feed Rate	Axial DOC
1	14.953	5.008	4.968
2	13.935	9.953	9.963
3	11.008	14.950	14.983
4	9.973	14.958	14.955
Delta	4.980	14.950	14.988
Rank	3	2	1

Table 4. 9: ANOVA for S/N Ratio of MRR

Source	DOF	SS	Mean Sum of Square	F	P	% Contribution
Material Density	3	0.010	0.003	5.72	0.034	0.00001
Feed Rate	3	325.836	108.612	193139.12	0.000	49.69
Da	3	329.935	109.978	195568.36	0.000	50.31
Residual Error	6	0.003	0.001			
Total	15	655.784				

4.4 Effect of process parameters on Change in Surface Roughness

The S/N ratio plot with main effects of each of the considered parameters for C/SiC composite are shown in Fig. 4.5 and Fig 4.6 respectively. The quality characteristic is of

'larger the better' type. The parameters that improve the material removal rate generally decrease the surface finish.

It is clear from the mean effect plot (Fig. 4.6) that change in surface roughness decreases with increase in material density, feed rate and axial depth of cut. With increase in the material density, hardness of the material increases so improvement in surface finish decreases. Increase in the feed rate and axial depth of cut increases the contact between the workpiece and tool which decrease the change in surface roughness.

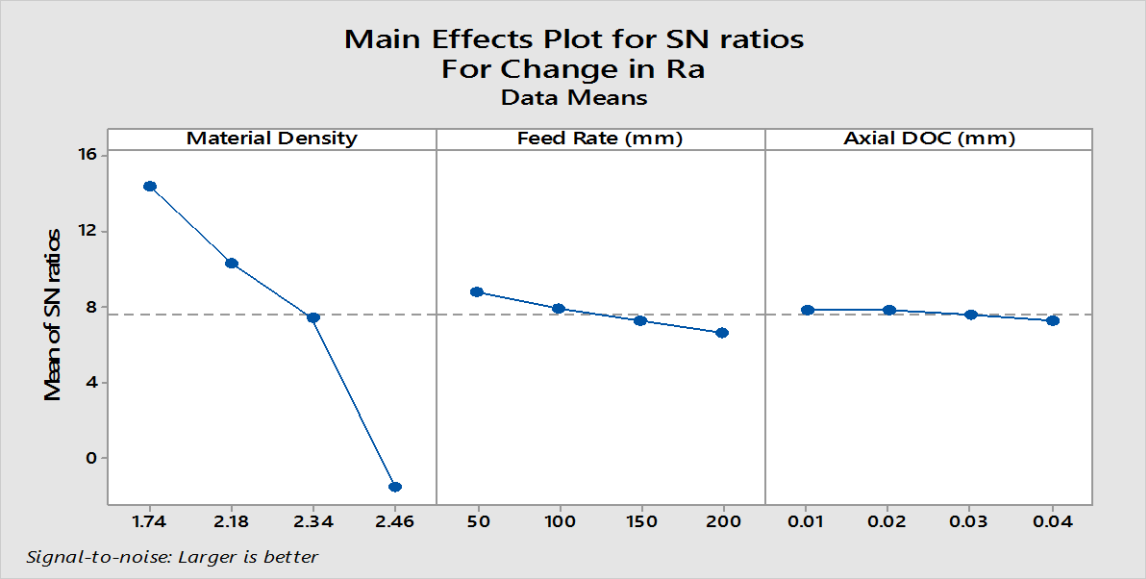

Fig. 4.5: SN ratio graph for change in Surface Roughness (R_a)

Fig. 4.6: Mean graph for change in Surface Roughness (R_a)

4.4.1 Selection of Optimal Levels:

With regarding to the S/N response, Fig. 4.5 clearly indicates that the first level of material density, feed rate and axial depth of cut has maximum value of change in surface roughness.

ANOVA table for S/N ratio (Table 4.12) shows that material density is the significant parameter for change in surface roughness while the effect of feed rate and axial depth of cut is negligible. The percentage contribution of material density was maximum i.e. 98.02 % while feed rate has 1.81 % and axial depth of cut has 0.16 %.

Hence maximum change in surface roughness was found in material of material density 1.74 g/cm^3 at feed rate of 50 mm/min and axial depth of cut is 0.01 mm.

Table 4.10 & 4.11 are the response table for S/N ratio and mean for the change in surface roughness. They shows the rank of the parameters. Change in surface roughness in RUM process is largely depends on material density than feed rate and minimum on axial depth of cut in the selected parameters.

Table 4. 10: Response Table for S/N ratio of change in Surface Roughness (Ra)

Level	Material Density	Feed Rate	Da
1	14.400	8.773	7.859
2	10.281	7.894	7.838
3	7.394	7.247	7.565
4	-1.534	6.628	7.279
Delta	15.934	2.146	0.580
Rank	1	2	3

Table 4.11: Response Table for means of change in Surface Roughness (Ra)

Level	Material Density	Feed Rate	Da
1	5.2825	3.3700	3.1525
2	2.2875	3.0450	3.0875
3	2.3500	2.7800	2.8400

4	0.8400	2.5650	2.6800
Delta	4.4425	0.8050	0.4725
Rank	1	2	3

Table 4. 12: ANOVA for S/N Ratio of change in Surface Roughness (Ra)

Source	DOF	SS	Mean Sum of Square	F	P	% Contribution
Material Density	3	547.568	182.523	20893.79	0.000	98.02
Feed Rate	3	10.113	3.371	385.88	0.000	1.81
Da	3	0.891	0.297	34.01	0.000	0.16
Residual Error	6	0.052	0.009			
Total	15	558.624				

4.6 Characterization of C/SiC:

Table 4.13: Composition of the sample

Element	**Weight %**	**Atomic %**
C	**45.77**	**66.37**
Si	**54.23**	**33.63**
Total	**100**	

Table 4.13 shows the Energy Dispersive X-ray microanalysis (EDS) result of sample. It shows that composite contains 45.77 % carbon and 54.23 % Silicon. Fig. 4.7 is the EDS image of the sample which graphically shows the containing elements in the sample.

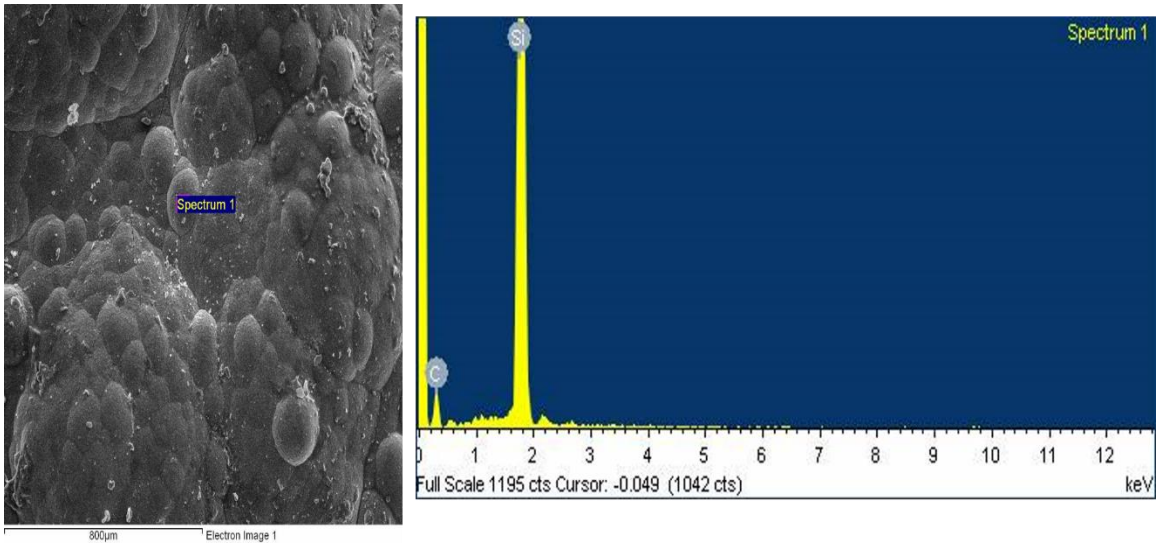

Fig. 4.7: EDS image of sample

Fig. 4.8 shows the scanning electron microscope (SEM) image of the cross section of the 2.49 g/cm^3 sample before the machining at 100 µm (a) and 500 µm (b). From photograph (a) and (b), shows the deposition of SiC around the carbon fibre. Silicon carbide was uniformly distributed between the gaps of C-fibre, which makes the strong bonding between carbon fibre and silicon carbide. This superior interfacial bonding increases the plastic deformation in the matrix which ultimately the cause for increase in the strength and toughness of composite.

Fig. 4.9 is the fractured image of C/SiC sample. It was clearly visible that single layer carbon and silicon carbide bonding was present on the composite. This shows that SiC was uniformly distributed throughout the sample and very less gap present inside the structure. This uniform distribution is the main reason behind the strength of the C/SiC composite and lesser gap make it more temperature resistant.

Fig. 4.10 is the SEM image which shows the orientation if C/SiC structure. It shows the needling technique which was used for the manufacturing of C/SiC composite. Fibres are placed with one layer at 0° and one at 90° and these layers are overlapping to each other.

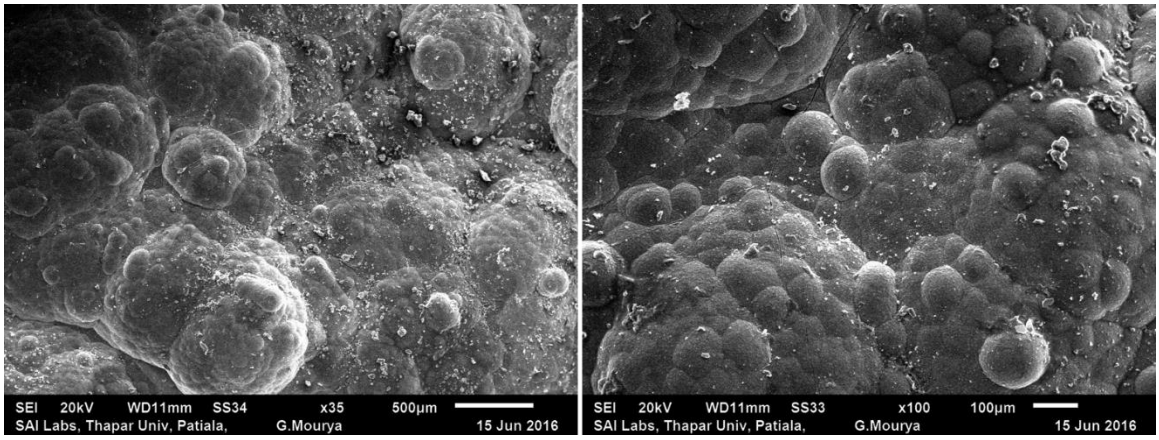

Fig. 4.8: SEM Image of 2.49 g/cm^3 sample before machining at (i) 100µm, (ii) 500 µm

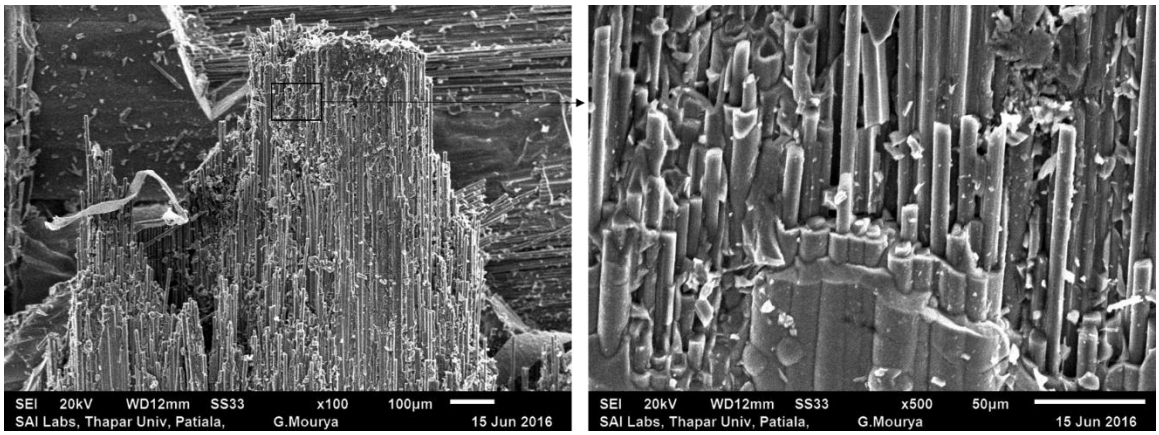

Fig. 4.9: Fractured image of C/SiC

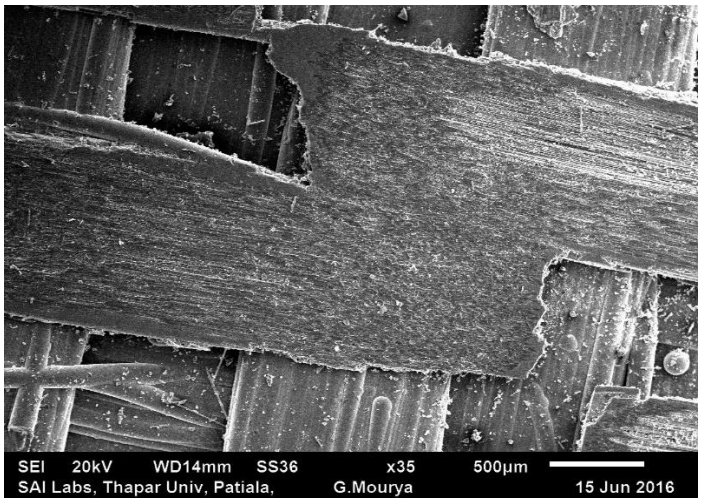

Fig. 4.10: SEM image for orientation of C/SiC composite

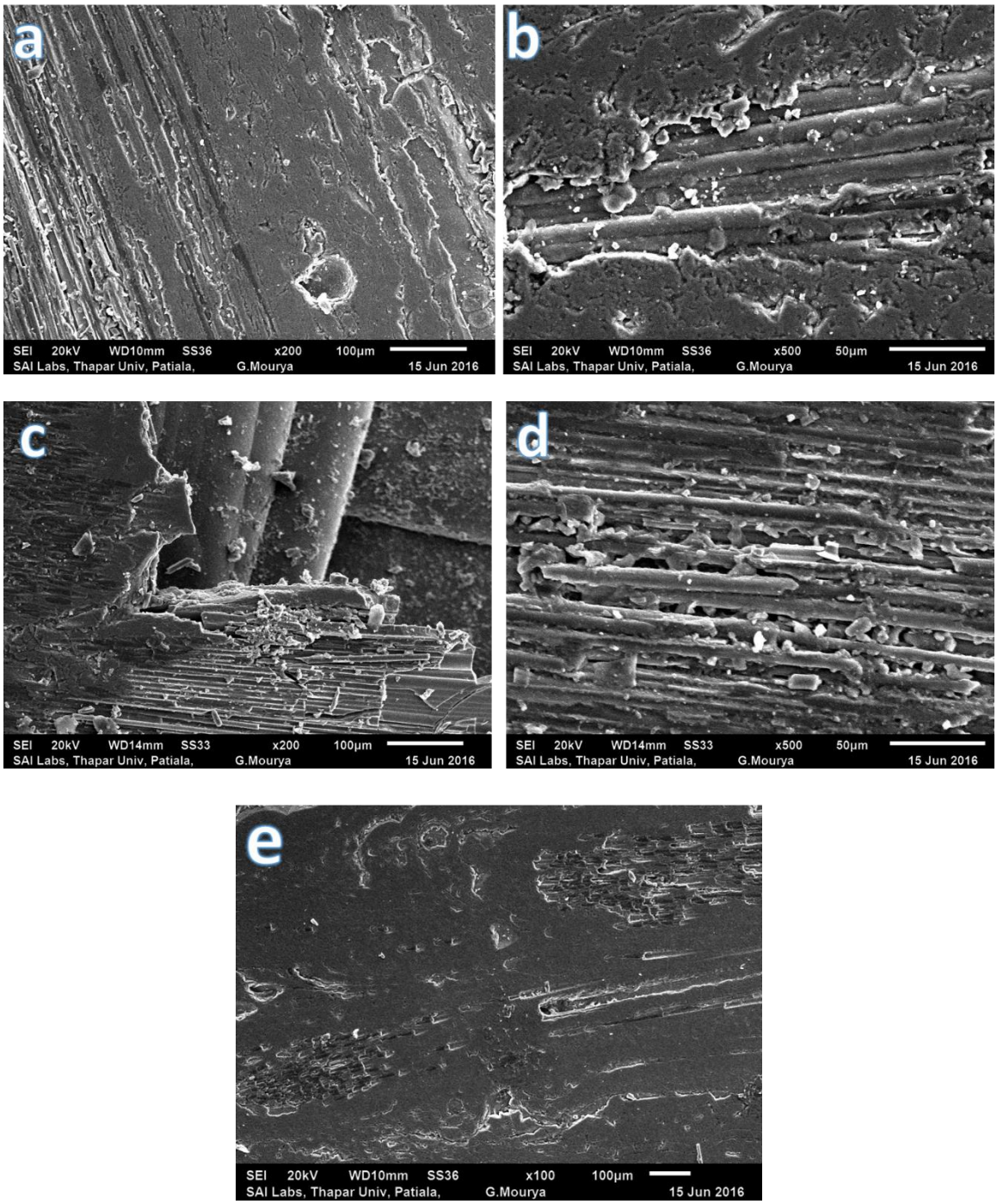

Fig. 4.11: SEM image after machining

Fig. 4.11 is the SEM image of C/SiC composite after rotary ultrasonic milling. Fig 'a' & 'b' are the image of C/SiC after machining with feed rate of 50 mm/min and 'c' & 'd' are after 150 mm/min feed rate. These images clearly indicates that the fibre pullout is more after machining with 150 mm/min compare to 50 mm/min. Fig. 'a', 'c' & 'e' also

shows that the direction of movement of milling tool is in the direction of fibre orientation. So material removal takes place on that direction. Fig. ‘e’ also shows some diamond grains of tool also impregnate onto the workpiece.

4.6 Analysis of Tool wear:

Tool length was measured before and after machining on each workpiece by Zoller Tool measure and presetter which was available at ‘AMF division, Vikram Sarabhai Space Center, ISRO Trivandrum. Decrease in tool length shows the linear tool wear. Tool length values are recorded in Table-4.13. As it clearly visible from table that decrease in tool length i.e. tool wear becomes lesser as the density of material reduces. This is because of decrease in matrix weight % of material with the decrease in density. So machining becomes easier.

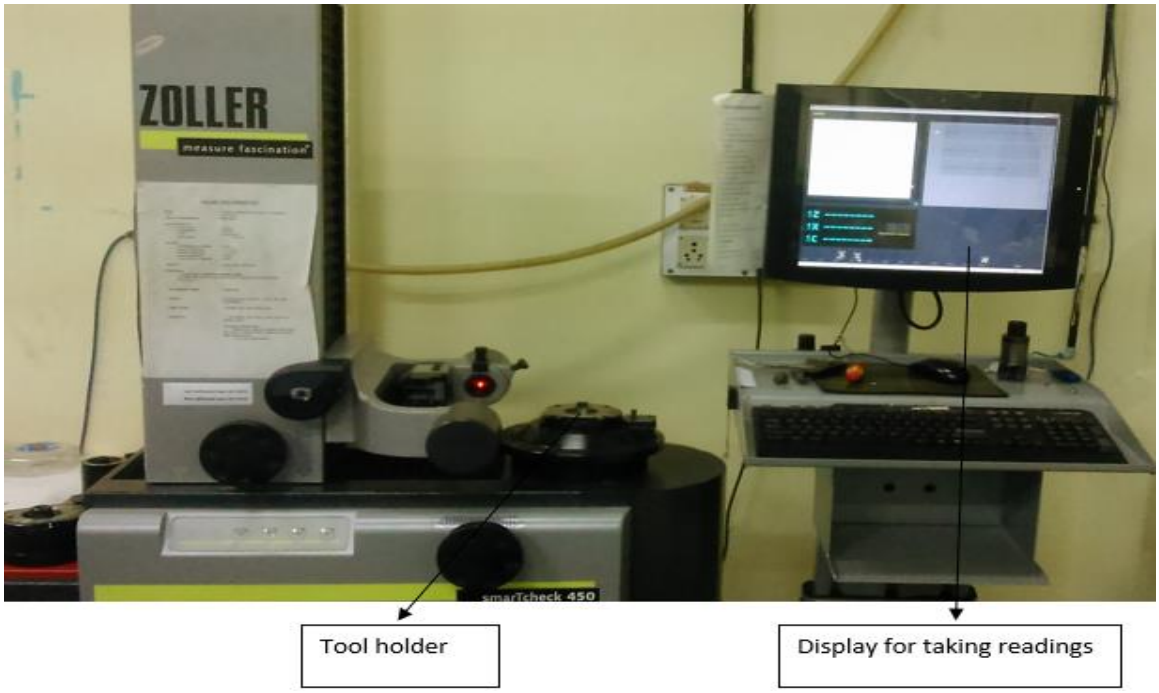

Fig. 4.12: Zoller tool measure and pre setter

Fig. 4. 13: Tool after machining

Table 4. 13: Decrease in Tool length after machining of each Workpiece

S. No.	Material Density	Tool Length Before Machining (mm)	Tool Length After Machining (mm)	Decrease in tool length (mm)
1	2.46	191.190	191.152	0.038
2	2.34	191.152	191.117	0.035
3	2.18	191.114	191.084	0.030
4	1.74	191.084	191.062	0.022

Chapter-5

CONCLUSION AND FUTURE SCOPE

5.1 Conclusion:

After studying the effect of input parameters such as material density, feed rate, axial depth of cut on torque exerted on tool, material removal rate and change in surface roughness during milling of C/SiC composite through rotary ultrasonic machining, the following conclusions are made:

1. All the parameters i.e. material density, feed rate, axial depth of cut have significant effect on torque exerted during rotary ultrasonic face milling of C/SiC. But axial depth of cut mostly affect the torque.
2. Torque is increases with the increase in material density, feed rate and axial depth of cut.
3. Minimum torque was generated onto the material with low material density at minimum feed rate and axial depth of cut.
4. With material density 1.74 g/cm^3, feed rate of 50 mm/min and axial depth of cut 0.01 mm; minimum torque was found.
5. Material removal rate is mainly affected by axial depth of cut and feed rate. Material density has negligible effect on the MRR
6. MRR is increases with the increase in axial depth of cut and feed rate.
7. Maximum MRR was found on material density composite 1.74 g/cm, at maximum feed rate 200 mm/min and axial depth of cut of 0.04 mm
8. Out of all selected parameters material density is predominant parameter responsible for change in surface roughness during rotary ultrasonic machining of C/SiC.
9. It was observed that maximum change in surface roughness was found in material with material density i.e. 1.74 g/cm^3 at fee rate of 50 mm/min and axial depth of cut of 0.01 mm.
10. From all the machining characteristics, it can be concluded that C/SiC with minimum material density is best for machining & application in aerospace

industry. As the density of C/SiC composite increases, machining becomes difficult.

11. The rate of Tool wear increases with the increase in material density of the C/SiC composite.

5.2 Scope for Future Work:

Although the present study, considers Rotary ultrasonic face milling of C/SiC composites but still there is a scope for further investigations considering the vast potential of this technique. The following suggestions is useful for future work.

1. In the present investigation, the effect of three input parameters i.e. material density, feed rate and axial depth of cut has been studied. Effect of other parameters like tool with different diameters, cutting speed, amplitude can also be included.
2. In the present study three output parameters are considered. Study of other responses such as force and type of chip formation can also be included.
3. In future, rotary ultrasonic drilling of C/SiC of different densities can also be taken for investigation of surface roughness as well as material removal rate.

REFERENCES

1. Hocheng, H., Tai, N.H., Liu, C.S., 2000, Assessment of ultrasonic drilling of C/SiC composite material, Compos. A 31, 133–142.
2. Zhao, K., Li, K., Wang, Y., 2013 Rapid densification of C/SiC composite by incorporating SiC nanowires, Compos. B 45, 1583-1586.
3. Bae, J.C., Cho, K.Y., Yoon, D.H., Baek, S.S., Park, J.K., Kim, J., Im, D.W., Riu, D.H., 2013, Highly efficient densification of carbon fiber-reinforced SiC-matrix composites by melting infiltration and pyrolysis using polycarbosilane, Cer. Intl. J. 39, 5623-5629.
4. Lee, D.H., Lee, E.J., Kim, J.C., Kim, D.J., 2014, Densification behavior of high purity SiC by hot pressing, Cer. Intl. J. 40, 16389-16392.
5. Ding, K., Fu, Y.C., Su, H., Chen, Y., Yu, X., Ding, G., 2014, Experimental studies on drilling tool load and machining quality of C/SiC composites in rotary ultrasonic machining, J. of Mat. Processing Tech. 214, 2900-2907
6. Krenkel, W., 2009, Design of ceramic brake, pad and disk", 26th Annual Conference on Composites, Ad. Cer., Mat. 9
7. Ortlet, N., Hald, H., Koch, D., 2015, CMC Rocket Thrust Chamber Technology Status and Perspectives, AIRBUS DS Space Systems 3 Technologies for Future Liquid Propulsion
8. Prabhakar, D., Ferreira, P.M., Haselkorn, M., 1992, An experimental investigations of material removal rates in rotary ultrasonic machining, Trans. Of American Society
9. Yang, W., Araki, H., Kohvama, A., Thaveethavorn, S., Suzuki, H., Noda, Tetsuzi, 2004, Fabrication in-situ SiC nanowires/SiC matrix composite by chemical vapour infiltration process, Mat. Letters 58, 3145-3148
10. Jacobsen, T.K., Bronsted, P., 2001, Mechanical properties of two plain-woven chemical vapor infiltrated silicon carbide-matrix composites, J. of American ceramic society
11. Oh, B.J., Lee, Y.J., Choi, D.J., 2001, Fabrication of Carbon/Silicon Carbide Composites by Isothermal Chemical Vapor Infiltration, Using the In Situ Whisker-Growing and Matrix-Filling Process, J. of American society

12. Nie, J., Xu, Y., Zhang, L., Cheng, L., Ma, J., 2009, Microstructure and tensile behavior of multiply needled C/SiC composite fabricated by chemical vapor infiltration, J. of Mat. Processing Tech. 209, 572-576
13. Taguchi, T., Nozawa, T., Lgawa, N., Katoh, Y., Jitsukawa, S., Kohyama, A., Hinoki, T., Snead, L.L., 2004, Fabrication of advanced SiC fiber/F-CVI SiC matrix composites with SiC/C multi-layer interphase, J. of Nuclear Mat., 572-576
14. Ma, J., Xu, Y., Zhang, L., Chemg, L., Nie, J., Dong, N., 2006, Microstructure characterization and tensile behavior of 2.5D C/SiC composites fabricated by chemical vapor infiltration, Scripta Materiala 54, 1967-1971
15. Vaidyaraman, S., Lackey, W.J., Freeman, G.B., Agrawal, P.K., Langman, M.D., 1995 Fabrication of carbon-carbon composites by forced flow-thermal gradient chemical vapor infiltration, J. of Mat. Research. Vol. 10 (6), 1469-1477
16. Caputo, A.J., Lackey, W.J., 1984, Fabrication of fibre reinforced ceramic matrix composite by chemical infiltration, Annual Conference on Comp. and Advanced Cer. 8
17. Okuno, H., Trinquecoste, M., Derre, A., Monthiouz, M., Delhaes, P., 2002, Catalytic effects on carbon/carbon composites fabricated by a film boiling chemical vapor infiltration process, J. of Mat. Research. Vol. 17, 1904-1913
18. Kadivar, M.A., Yousefi, R., Akbari, J., Rahi, A., Nikouei, S.M., 2012, Burr Size Reduction in Drilling of Al/SiC Metal Matrix Composite by Ultrasonic Assistance, Advanced Mat. Research. Vol. 410, 279-282
19. Kadivar, M., Akbari, J., Azghandi B.V., 2014, Investigating the effect of ultrasonic vibration on hole accuracy in drilling of metal matrix composites, Advanced Mat. Research. Vol. 966-967,137-141
20. Mehbudi, P., Baghlani, V., Akbari, J., Bushroa, A.R., Mardi, N.A., 2013, Applying ultrasonic vibration to decrease drilling-induced delamination in GFRP laminates, Procedia CIRP 6, 577-582
21. Abdo, B.M.A., Darwish, S.M., Tamimi, A.M.E., 2012, Parameters Optimization of Rotary Ultrasonic Machining of Zirconia Ceramic for Surface Roughness Using Statistical Taguchi's Experimental Design, Applied Mech. And Mat. Vol.184-185, 11-17

22. Navas, V.G., Sanda, A., Sanz, C., Fernandez, A., 2015, Surface Integrity of rotary ultrasonic machined ZrO_2-TiN and Al_2O_3-TiC-SiC ceramics, J. of European Cer. Society 35(14), 3297-3941
23. Liu, Y., Wang, C., Li, W., Zhang, L., Yang, X., Cheng, G., Zhang, Q., 2014, Effect of energy density and feeding speed on micro-hole drilling in C/SiC composites by picosecond laser, J. of Mat. Processing Technology 214, 3131-3140
24. Caroll, J.W., Todd, J.A., Laser machining of ceramic matrix composites, Dept. of Mechanical, Illinois institute of technology, USA (312), 567-8867
25. Wang, C., Zhang, L., Liu, Y., Zhang, Q., Hua, K., 2013, Ultra-short pulse laser deep drilling of C/SiC composites in air, Appl. Physics 111, 1213-1219
26. Zhang, L., Ren, C., Ji, C., Wang, Z., Chen, G., 2016, Effect of fiber orientations on surface grinding process of unidirectional C/SiC composites, Applied Surface Science 366, 424-431
27. Wang, T., Xie, L.J., Wang, X.B., Jiao, L., Shen, J.W., Xu, H., Nie, F.M., 2013, surface integrity of high speed milling of Al/SiC/65p aluminium matrix composite, CIRP Vol. 8, 475-480
28. Abdo, B.M.A., Darwish, S.M., Tamimi, A.M.E., Ahmari A.M., 2015, Experimental Investigation of Cutting Forces in Ti-6Al-4V Alloys Using Rotary Ultrasonic Machining, Intl. Conference on Aeronautical, Robotics and Manufacturing Engineering
29. Li, Z.C., Jiao, Y., Deines, T.W., Pei, Z.J., Treadwell, C., 2005, Rotary ultrasonic machining of ceramic matrix composites: feasibility study and designed experiments, Intl. J. of Machine Tools & Manufacture 45, 1402-1411.
30. Nik, M.G., Mohvahhedy, M.R., Akbari, J., 2012, Ultrasonic-Assisted Grinding of Ti6Al4V Alloy, Procedia CIRP 1, 353 – 358
31. Bertsche, E., Ehmann, K., Malukhin, K., 2013, Ultrasonic slot machining of a silicon carbide matrix composite, Int J. Adv Manuf. Tech. 66, 1119-1134
32. Jiao, Y., Liu, W.J., Pei, Z.J., Xin, X.J., Treadwell, C., 2005, Study on Edge Chipping in Rotary Ultrasonic Machining of Ceramics: An Integration of Designed Experiments and Finite Element Method Analysis, J. of Manufacturing Science and Engineering

33. Zhao, C.Y., Gong, H., Fang, F.Z., Li, Z.J., 2013, Experimental study on the cutting force difference between rotary ultrasonic machining and conventional diamond grinding of K9 glass, Machining Science and Technologu 17, 129-144
34. Prever, B., Signorelli, Denaro, Camarri, Vita, D., 2013, TPS Design, Development and Verification Approach for IXV Program, Intl. Experimental Vehicle 15